Int. J. Human–Computer Studies 183 (2024) 103200

Contents lists available at ScienceDirect

International Journal of Human - Computer Studies

journal homepage: www.elsevier.com/locate/ijhcs

Pedestrians' road-crossing decisions: Comparing different drift-diffusion models

Max Theisen [a], Caroline Schießl [a], Wolfgang Einhäuser [b], Gustav Markkula [c,*]

[a] Institute of Transportation Systems, German Aerospace Center (DLR), Lilienthalplatz 7, 38108 Braunschweig, Germany
[b] Institute of Physics, Chemnitz University of Technology, Reichenhainer Straße 70, 09126 Chemnitz, Germany
[c] Institute for Transport Studies, University of Leeds, 34-40 University Road, Leeds LS2 9JT, UK

ARTICLE INFO

Keywords:
Cognitive modelling
Decision-making
Drift-diffusion model
Pedestrian–vehicle interaction
Pedestrian crossing

ABSTRACT

The decision of whether to cross a road or wait for a car to pass, humans make frequently and effortlessly. Recently, the application of drift-diffusion models (DDMs) on pedestrians' decision-making has proven useful in modelling crossing behaviour in pedestrian–vehicle interactions. These models consider binary decision-making as an incremental accumulation of noisy evidence over time until one of two choice thresholds (to cross or not) is reached. One open question is whether the assumption of a kinematics-dependent drift-diffusion process, which was made in previous pedestrian crossing DDMs, is justified, with DDM-parameters varying over time according to the developing traffic situation. It is currently unknown whether kinematics-dependent DDMs provide a better model fit than conventional DDMs, which are fitted per condition. Furthermore, previous DDMs have not considered reaction times for the not-crossing option. We address these issues by a novel experimental design combined with modelling. Experimentally, we use a 2-alternative-forced-choice paradigm, where participants view videos of approaching cars from a pedestrian's perspective and respond whether they want to cross before the car or to wait until the car has passed. Using these data, we perform thorough model comparison between kinematics-dependent and condition-wise fitted DDMs. Our results demonstrate that condition-wise fitted DDMs can show better model fits than kinematics-dependent DDMs as reflected in the mean-squared-errors. The condition-wise fitted models need considerably more parameters, but in some cases still outperform kinematics-dependent DDMs in measures that penalize the parameter number (e.g., Akaike information criterion). Introducing a starting point bias provides support for the novel hypothesis of rapid early evidence build-up from the initial view of the vehicle distance. The drift rates obtained for the condition-wise fitted models align with the assumptions in the kinematics-dependent models, confirming that pedestrians' decision processes are kinematics-dependent. However, the partial preference for condition-wise fitted models in the model selection suggests that the correct form of kinematics-dependence has not yet been identified for all DDM-parameters, indicating room for improvement of current pedestrian crossing DDMs. Developing more accurate models of human cognitive processes will likely facilitate autonomous vehicles to understand pedestrians' intentions as well as to show unambiguous human-like behaviour in future traffic interactions with humans.

1. Introduction

As of 2023, autonomous vehicles (AVs) are still no reality for public users with the exception of ride-hailing services in few selected places (Schwall et al., 2020). Expectations of the deployment of AVs to the public market in the last ten years have not been reached (cf. Litman (2013, 2022)). One remaining problem is the control of AVs in crowded urban areas (Schwarting et al., 2018; Rasouli and Tsotsos, 2019), where AVs need to simultaneously interact with multiple human drivers and with vulnerable road users (VRUs; e.g., pedestrians, cyclists), who are less likely to stick to predefined paths or obey traffic rules. To adequately interact with humans (vehicle drivers or VRUs), the AV should predict their intentions and adapt its own actions accordingly. In turn, the AV itself should show human-like behaviour to help humans understand the AV's own motion intentions (Li et al., 2018). Both to predict and to show human-like behaviour, it can be beneficial to approximate the cognitive processes underlying human behaviour in the form of cognitive models (Markkula and Dogar, 2022).

* Corresponding author.
E-mail address: g.markkula@leeds.ac.uk (G. Markkula).

https://doi.org/10.1016/j.ijhcs.2023.103200
Received 30 January 2023; Received in revised form 21 November 2023; Accepted 28 November 2023
Available online 30 November 2023

In the present study, we consider a specific case of human behaviour in traffic, the decision as to whether and when to cross a road in front of an oncoming vehicle. In this scenario multiple factors can influence the pedestrian's crossing decision, for example, the vehicle's static appearance (type, colour, size) and dynamic factors (time gap, speed, distance, communication to pedestrians), physical context (street width, number of lanes, weather), social factors (group size, age, gender, culture) or the pedestrian's state (walking speed, waiting time, attention) (Rasouli and Tsotsos, 2019). In this study, we focus on pedestrians' (time) gap acceptance and how it is influenced by different vehicle speeds, a subject that has already been studied extensively (Oxley et al., 2005; Lobjois and Cavallo, 2007; Schmidt and Faerber, 2009; Petzoldt, 2014). These studies have shown that pedestrians do not behave optimally in that they are more likely to cross a road at smaller critical time gaps if a vehicle approaches with higher speeds, leaving less avoidance time in case of an error (which is especially critical given the non-linear relationship between velocity and kinetic energy in a potential collision). Some previous gap acceptance models have used a logistic regression to model pedestrians' crossing behaviour (Zhao et al., 2019; Tian et al., 2022). For the use case of AVs, it is, however, crucial to dynamically estimate the decision process of a pedestrian throughout the interaction. Extending beyond previous studies, we therefore consider cognitive models of road crossing that adapt their parameters to the kinematic variables of the interaction and compare them to static models. Specifically, we consider different cases of drift-diffusion models (DDMs, Ratcliff and McKoon (2008)), which have the additional advantage that their parameters can be readily interpreted and therefore provide insight in the temporal evolution of the pedestrian's decision process. On the experimental side, we enable testing these models by not only querying the time point of a positive crossing decision (go/no-go task), but also the time point of a negative crossing (waiting) decision by using a 2-alternative-forced choice (2-afc) paradigm; that is, participants have to respond in any case, either to cross or to wait.

Originally introduced by Ratcliff (1978), the DDM describes decision situations with two alternative options, in our case a pedestrian deciding whether or not to cross a road in front of an oncoming vehicle. The model assumes that evidence is accumulated incrementally over time until one of two thresholds is reached, at which point the corresponding decision (e.g., crossing or waiting) is considered made. In its simplest form the DDM consists of four parameters (see Fig. 1):

- the mean drift rate ξ (reflecting the speed at which evidence accumulates for one option over the other — the higher the more confident the decision-maker)
- the boundary separation a (reflecting the amount of accumulated evidence needed to make a decision — the higher the more cautious the decision-maker)
- the non-decision time T_{er} (reflecting the part of reaction time that is unrelated to decision-making, e.g., perception and motor execution)
- the starting point bias z (reflecting the decision-maker's tendency to favour one option over the other from the start), which in the symmetric case of $z = 0$ effectively reduces the *basic DDM* even further to a 3-parameter model

It is assumed that the evidence accumulation process is stochastic, so additionally a noise parameter s (reflecting the fluctuations in the evidence accumulation process) needs to be specified, which is conventionally kept constant to scale all other parameters ($s = 1$ in our case). The 4-parameter *basic DDM* was later extended to the 7-parameter *full DDM* by Ratcliff and Rouder (1998), Ratcliff and Tuerlinckx (2002) in order to allow for the inter-trial variabilities of drift rate η, non-decision time s_t and starting point bias s_z. Thereby, potential differences in the speed of response of choices A and B (in our case, crossing and waiting) can be explained (Lerche and Voss, 2016).

DDMs are often applied to situations where within a trial the stimulus parameters do not vary over time, such that the amount of evidence that can be accumulated per unit time remains constant. In these cases, DDM parameters are fitted condition-wise, as within a condition parameters do not vary. In the pedestrian crossing task, in contrast, the available information changes over the course of a trial as the car approaches the pedestrian. Hence, several previous studies that have applied DDMs to the road crossing task (e.g., Markkula et al. (2018), Giles et al. (2019) and Pekkanen et al. (2022)) have fitted their models across conditions, with situation kinematics determining DDM parameters (e.g., drift rate, boundary separation) in the individual experimental conditions. The same applies for Zgonnikov et al. (2022) who addressed left-turning before or after an oncoming vehicle and tested the Giles et al. (2019) model but also introduced a new model with collapsing boundaries which has not been tested for pedestrian crossing yet.

Therefore, these models have taken quite a large conceptual leap from the conventional DDMs introduced by Ratcliff (1978), and it has not been strictly shown that all those changes were motivated and indeed improve the models' predictive performance. To compare such models to simpler models is particularly relevant as for the case of condition-wise fits, less complex DDMs can outperform full 7-parameter DDMs, especially if the number of trials is low (Lerche and Voss, 2016). It remains an open question whether this is also the case for a more complex task where the stimulus information available to the user varies over a trial, such as in a pedestrian crossing task. We try to fill this gap by connecting the pedestrian crossing DDMs back to their roots in the conventional DDMs — in terms of the fitting procedure, rigorous model comparisons and an adapted experimental approach. Specifically, we compare DDMs with kinematics-dependent and kinematics-independent drift rates and boundary separations in terms of goodness-of-fit (mean squared error — MSE) and model quality regarding simplicity (Akaike information criterion — AIC and Bayesian information criterion — BIC). We compare model fits that include the condition (condition-wise fits) to fits that are not given the condition explicitly (but implicitly through the kinematic parameter settings). Whereas earlier studies on traffic-related interactions (e.g., Markkula et al. (2018), Giles et al. (2019), Zgonnikov et al. (2022) and Pekkanen et al. (2022)) focused on crossing decisions and thereby disregarded 50% of the information (the timing of the waiting decision), we here treat crossing and waiting decisions symmetrically. This required the collection of new experimental data, which allow us to test the DDMs to their full extent. As such, our contribution is two-fold: on the modelling side, we provide a rigorous comparison of DDM models of varying complexity for the pedestrian crossing task, on the experimental side, we provide a novel dataset that makes the otherwise covert waiting decision experimentally accessible.

2. Methods

2.1. Experiment

Participants

135 participants (65 male, 69 female, 1 did choose to not state their gender) aged between 18 and 80 years took part in the online experiment ($M = 37.6$ years, SD = 16.9 years). The recruiting procedure specifically targeted individuals experienced in psychophysical and/or traffic psychology experiments. Study participants were recruited via the participant pool of the Institute of Transportation Systems of the DLR and via a mailing list dedicated to recruit participants of the TU Chemnitz. All participants had normal or corrected to normal vision and participated voluntarily. Each participant received course credit for the duration of the experiment or the opportunity to take part in the draw for a voucher. An ethical review application was submitted to the ethics commission of the DLR. The ethics commission stated that there is no relevance for an assessment and decided to waive the requirement of an in-depth ethical review for this study.

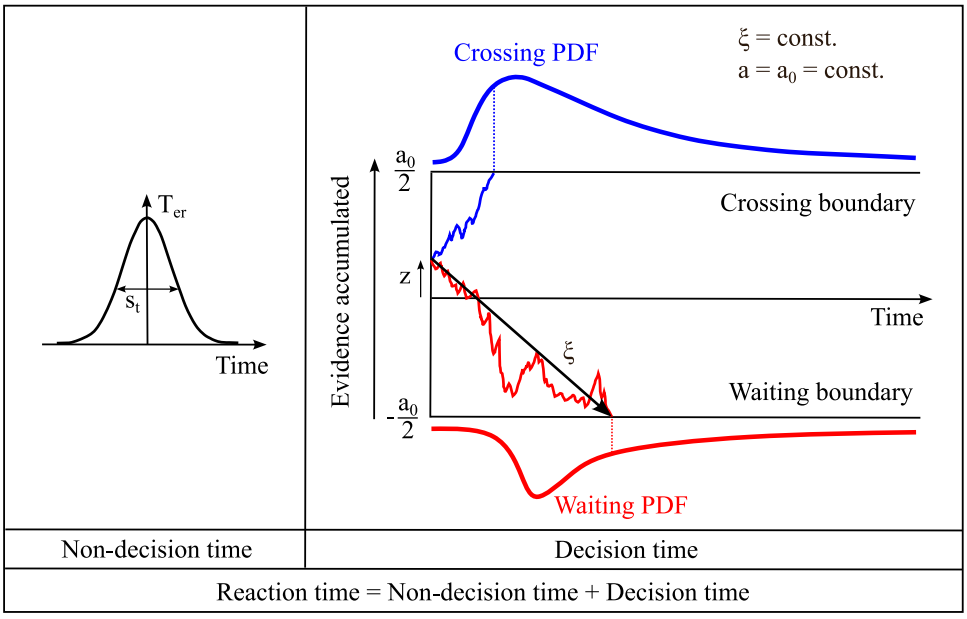

(a) Condition-wise fitted model with time-invariant drift rate ξ and boundary separation a

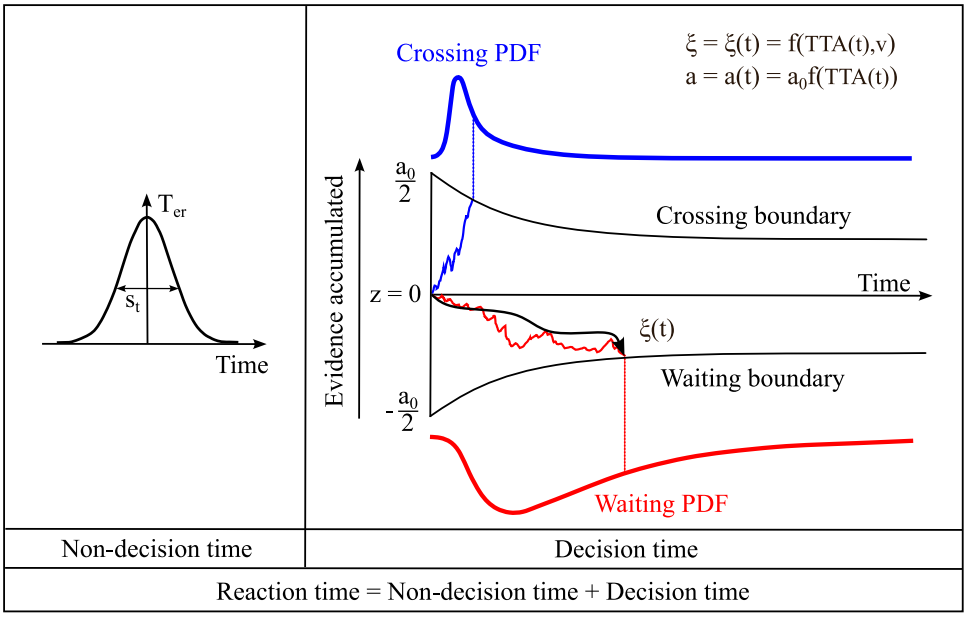

(b) Kinematics-dependent model with time-dependent drift rate $\xi(t)$ and boundary separation $a(t)$

Fig. 1. Schematic representation of the different DDMs for the road-crossing task compared in this paper including exemplary crossing and waiting probability density functions (PDFs).
Source: Adapted after Wagenmakers et al. (2007), Farrell and Lewandowsky (2018) and Zgonnikov et al. (2022).

Procedure

The participants were instructed to take the role of a pedestrian standing at the roadside of an urban road (without zebra crossing or traffic lights) who wants to cross the road (see Fig. 2). Furthermore, the participants were told that in each trial of the experiment a single car would be driving towards them with constant speed on the right side of the road. It was stated that the left side of the road was always clear to cross. In the experiment the participants had to decide whether they would cross the road in front of the oncoming vehicle or would not cross the road and wait until the car had passed by. The participants were instructed to use their index fingers to report their decision outcome (crossing or waiting) with the orientation keys F and J and to use their thumbs to start the next trial with the space bar. We counterbalanced the assignment of the keys, so half of the participants reacted with F to cross and J to wait and the other half with J to cross and F to wait.[1] Participants were instructed to react as fast as possible and keep their hands in the position at any time during the experiment.

[1] In practice, this was done by alternating the assignment, such that for the odd number of participants there was in fact one more of the former assignments.

Fig. 2. Screen shot of the video stimulus material generated with CARLA simulator (Dosovitskiy et al., 2017). For example videos see Appendix B.

Design

The experiment used a 7 × 3 within-subject design with the car's time-to-arrival (TTA) and velocity[2] as independent variables. The TTA was measured as the time that the car needs to travel from its position in the first frame of the video until it reaches the position of the pedestrian. We varied the TTA between 2 s and 8 s in steps of 1 s. Regarding the car's velocity we used three different conditions that are typical for urban traffic: 20, 40 and 60 km/h. Since constant velocities were used, our independent variables v and TTA are inversely proportional to each other, connected via the distance d between vehicle and pedestrian:

$$v = \frac{d}{TTA} = const. \tag{1}$$

The video and the trial ended as soon as the participants reacted with one of the orientation keys (i.e., the video turned to a white screen and the next trial could be started with the space bar). If the participants did not press a button, the trial ended by itself after the car had passed. There was no feedback provided to the participants whether the crossing was successful or not. The experiment consisted of a training block with 7 trials and three blocks of 21 trials so that each possible combination of TTA and velocity was repeated once per block. The order of trials in each block was random.

Materials

The participants performed the experiment on their own computer. The web-browser-based experiment was created using jsPsych (De Leeuw, 2015) and the video stimulus material was generated with CARLA simulator (Dosovitskiy et al., 2017). The videos were presented with a frame rate of 30 Hz and a resolution of 1280 × 720 px. Compared to a laboratory study there are more sources of variability to be regarded, since the experiment is performed with different hardware and software for each participant. For the measurement error of the reaction times we have to consider the trial-to-trial variability and the computer-to-computer variability (lag) of different hardware and software sources, most importantly keyboard, browser and platform (Bridges et al., 2020). Different USB-keyboards can have quite different latencies (lag) of roughly 15 to 60 ms (Luu, 2017), whereas the trial-to-trial variability is typically below 10 ms. According to Bridges et al. (2020) also the combination of different computer platforms (e.g., Win10, macOS, Ubuntu) and internet browsers (e.g., Chrome, Firefox, Safari, Edge) used together with jsPsych introduce an additional lag of 15 to 55 ms and a trial-to-trial variability of up to 10 ms. Since the different error sources are additive the total (maximum) error of the reaction time measurement adds up to 115 ms in lag and 20 ms in trial-to-trial variability. Since we use a within-subject design the absolute lag is additive and is subtracted out in the between-condition within-subject comparison, such that only the trial-to-trial variability limits precision. This possible 20 ms trial-to-trial variability needs to be borne in mind when interpreting the results. In our model, the variance-in-non-decision-time parameter s_t can capture this variability in trial-to-trial-delays.

2.2. Modelling

Model implementation

To analyse the participants' decision-making, we used the drift-diffusion modelling framework PyDDM (Shinn et al., 2020) (Details can be found in Appendix A). We employed maximum likelihood estimation as the fitting method to estimate the parameters of the DDM. We compared the three kinematics-dependent models introduced in the supplementary information of Zgonnikov et al. (2022) with four conventional DDMs that we fitted condition-wise to an aggregated set of all participants. Instead of fitting a separate model to each participant, we aggregated the data for the condition-wise fitted and kinematics-dependent models over all participants because there were too few observations per participant and condition. In practice, this amounts to the simplifying assumption that all participants are the same — an assumption that was already made by previous pedestrian crossing models (Pekkanen et al., 2022). According to Lerche and Voss (2016) especially across-trial variability in drift rate η and starting point s_z are typically estimated less accurately than the other DDM

[2] Intuitively, one might assume that velocity explains no additional variance/information beyond TTA (which combines information on velocity and distance). However, previous studies have found that velocity, even though it should not guide pedestrians' choice, has an impact beyond what TTA explains (Oxley et al., 2005; Lobjois and Cavallo, 2007; Schmidt and Faerber, 2009; Petzoldt, 2014). Therefore, we believe that it is relevant to assess velocity independently, despite its apparent redundancy. Additionally, velocity – given constant TTAs – can be seen as a proxy for initial distance (for identical TTAs, a faster car will be further away).

parameters (Vandekerckhove and Tuerlinckx, 2007; van Ravenzwaaij and Oberauer, 2009; Lerche et al., 2017). Therefore, following previous road-crossing models, we assume that for all models across-trial variability in drift rate ($\eta = 0$) and in starting point ($s_z = 0$) are zero. Additionally, for all kinematics-dependent models we assume that there is no starting point bias towards one decision boundary ($z = 0$), as this was the case in previous pedestrian crossing models.

Model comparison

For the kinematics-dependent models, one model is computed for all experimental data. The kinematics-dependent models are (see grey rows in Table 1):

- **8-parameter-Zgonnikov-DDM** (after Zgonnikov et al. (2022)): A dynamic drift rate $\xi(t)$ depending on TTA and speed v of the oncoming car:

$$\xi(t) = \alpha\left[TTA(t)\left(1+\beta v\right) - \theta\right] \tag{2}$$

  with the drift-rate-scaling-parameter α, the TTA-and-speed-weighting-parameter β, a critical parameter θ and a dynamic decision boundary $a(t)$ depending on the time-to-arrival $TTA(t)$ of the oncoming vehicle at time t:

$$a(t) = \frac{a_0}{1 + e^{-k\left(TTA(t)-\tau\right)}} \tag{3}$$

  with the boundary-scaling-parameter a_0, the TTA-sensitivity-parameter k and the time gap τ where the boundary is at its baseline value and a Gaussian-distributed non-decision time with mean T_{er} and variance s_t.
- **6-parameter-Giles-DDM** (after Giles et al. (2019)): A dynamic drift rate $\xi(t)$ depending on TTA and speed v of the oncoming car according to Eq. (2), a constant decision boundary a and a Gaussian-distributed non-decision time with mean T_{er} and variance s_t.
- **6-parameter-Ratcliff-DDM** (after Ratcliff (1978)): A static drift rate ξ determined by the speed v of the oncoming car and its time-to-arrival $TTA_{t=0}$ at the start of the video:

$$\xi = \alpha\left[TTA_{t=0}\left(1+\beta v\right) - \theta\right] \tag{4}$$

  and a constant decision boundary a and a Gaussian-distributed non-decision time with mean T_{er} and variance s_t.

For the condition-wise fitted models, one model is computed per TTA/velocity condition. In order to compare the results with the kinematics-dependent models, the MSE, AIC and BIC values of a combined model are computed by testing how well the sub-models for each TTA/velocity condition explain the combined data-set. The condition-wise fitted models are (see white rows in Table 1):

- **3-parameter-DDM**: A constant drift rate ξ, a constant decision boundary a, and a constant non-decision time T_{er} are fitted per condition.
- **4-parameter-DDM (ND-time variance)**: A constant drift rate ξ, a constant decision boundary a, and a Gaussian-distributed non-decision time with mean T_{er} and variance s_t are fitted per condition.
- **4-parameter-DDM (Starting point)**: A constant drift rate ξ, a constant decision boundary a, a constant non-decision time T_{er} and a constant starting point z are fitted per condition.
- **5-parameter-DDM**: A constant drift rate ξ, a constant decision boundary a, a Gaussian-distributed non-decision time with mean T_{er} and variance s_t and a constant starting point z are fitted per condition.

3. Results

3.1. Experiment

135 participants each performed 63 trials accounting for 8505 total trials. We excluded every trial where the participant reacted only after the car had passed by the exact position of the camera recording the scene. If this happened in more than 10% of a participant's trials, we excluded the whole data-set assuming that the participant did not understand the task correctly or did not pay enough attention to the experiment. We therefore completely excluded the data of 3 participants according to that criterion, reducing the data to 8316 trials. If it happened less often, we only excluded the trial as an outlier, keeping the rest of the data-set of the participant (8289 trials left). Additionally, we used skew-adjusted boxplots to identify trial outliers for each condition with the lengths of the upper and lower whiskers according to Hubert and Vandervieren (2008). This mostly excluded long reaction times that are likely due to an attentional lapse rather than a decision-making process. This reduced the total data further down to 7859 trials (92% of the original data). Next to reaction time we also checked if any participants seemed to randomly choose between crossing and waiting. As accuracy criterion, we verified that all participants would cross the road more often for high TTAs (6–8 s) than low TTAs (2–4 s). In doing so, we identified two individuals that did not meet this criterion and therefore were excluded, but this exclusion did not affect the interpretation of the model results. This reduced the total data further down to 7777 trials (91% of the original data), which is the final data-set for all further modelling and calculations. This led to reaction times between 0.37 s and 2.34 s. Provided the reaction-time and accuracy data, we have no reason to assume that any of the participants applied some kind of inappropriate fast-guessing strategy to finish the experiment quickly; rather, all seemed to have complied with task instructions.

Our results show that, given a constant approaching velocity, a bigger time gap of the car also leads to a bigger willingness to cross the road for the pedestrian (see Fig. 3, left side). The probability of gap acceptance for different vehicle speeds is qualitatively in line with previous studies since higher vehicle speeds at constant TTA lead to a higher gap acceptance and a similar relationship between crossing probability and distance for different vehicle speeds (e.g., Lobjois and Cavallo (2007) and Tian et al. (2022)). So, for the same time gap, pedestrians were more likely to cross the road the faster the approaching car was driving. Even though it is counterintuitive at first, it is well known that pedestrians are more likely to cross in front of faster cars (given constant TTA, see e.g. Oxley et al. (2005), Lobjois and Cavallo (2007), Schmidt and Faerber (2009) and Petzoldt (2014)), presumably because they overly base their decision on distance (faster cars are further away given constant TTA) rather than TTA alone. That is why we think that it could be possible that higher velocities (given constant TTA) at least to some extend lead to higher biases towards the crossing option. Quantitatively, gap acceptance in our study was slightly more conservative, presumably because participants had to cross a two-lane road, whereas most previous studies focused on one-lane roads. If participants were ideal observers, only TTA should matter for the crossing decision. We replicate this observer-bias, even though we have changed two things compared to previous experiments (two response buttons and conducting the experiment online). The difference is most prominent for medium time gaps. For example, if the car started appearing 5 s away driving at 60 km/h, pedestrians decided to cross the road in 76% of cases but only in 34% if the car was driving 20 km/h. These results indicate that the paradigm was successful in eliciting typical pedestrian crossing behaviour that is in line with that observed in previous studies. Regarding reaction times we find that in all velocity conditions, participants decided fastest ($\approx 0.8 - 1.0$ s) if the car appeared closest to them (TTA of 2–3 s). Interestingly, for bigger time gaps the reaction time increased until a maximum of $\approx 1.2 - 1.5$ s for medium time gaps of 5–6 s, until it

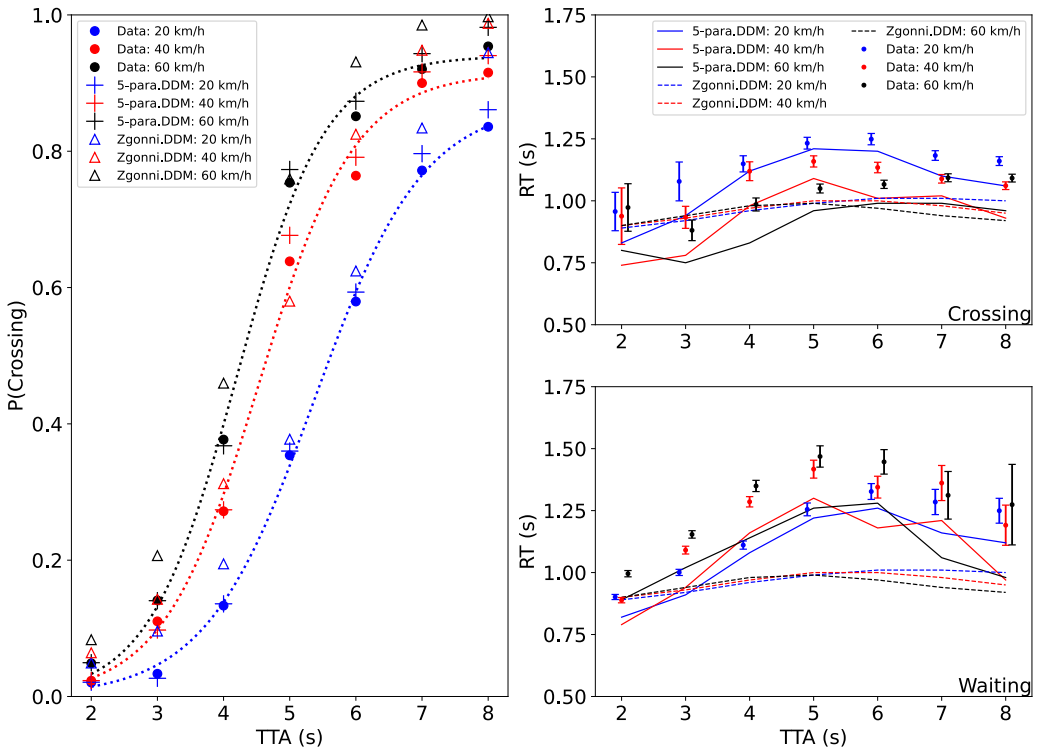

Fig. 3. Crossing decisions observed in the online experiment compared to the best-performing condition-wise fitted (5-parameter DDM) and kinematics-dependent model (Zgonnikov-DDM). Left side: Crossing probability data (round markers) for different time gaps and velocities of the car averaged over all participants supplemented by a sigmoidal trend as a guide-to-the-eye (dotted line) and model predictions of the 5-parameter DDM (crosses) and the Zgonnikov-DDM (triangles). Right side: Reaction times for different time gaps and velocities of the car averaged over all participants separated after crossing (top) and waiting (bottom) decision outcome. Error bars show standard errors of the mean. Solid lines show the prediction of the 5-parameter DDM, dashed lines show the Zgonnikov-DDM.

Table 1
Model comparison of different DDMs fitted to our data. Models with kinematics-dependent parameters (drift rate, boundary separation) are indicated by a grey background. Condition-wise fitted models without explicitly assumed kinematics-dependent parameters are indicated by a white background. Numbers in parentheses indicate the number of parameters that were fitted per column of Table 1, adding up to the total number of parameters per DDM indicated in the second column. *Static* means that constant values were fitted, *dynamic* means that varying time-dependent values were fitted for each trial. Best performing (smallest) MSE, AIC and BIC values are indicated by a green background.

Model name	Parameters	Drift rate	Boundary separation	Starting point	ND-time mean	ND-time variance	MSE	AIC	BIC
Ratcliff-DDM in Zgonnikov et al. (2022)	6	Static, kin. dep. (3)	Static (1)	0	Static (1)	Static (1)	0.070	9780	9822
Giles-DDM in Zgonnikov et al. (2022)	6	Dynamic, kin. dep. (3)	Static (1)	0	Static (1)	Static (1)	0.070	9665	9707
Zgonnikov-DDM in Zgonnikov et al. (2022)	8	Dynamic, kin. dep. (3)	Dynamic, kin. dep. (3)	0	Static (1)	Static (1)	0.065	9470	9526
Cond.-wise fitted 3-param. DDM	63	Static (21)	Static (21)	0	Static (21)	0	0.062	10 868	11 306
Cond.-wise fitted 4-param. DDM (ND-time variance)	84	Static (21)	Static (21)	0	Static (21)	Static (21)	0.059	9215	9800
Cond.-wise fitted 4-param. DDM (Starting point)	84	Static (21)	Static (21)	Static (21)	Static (21)	0	0.060	10 127	10 712
Cond.-wise fitted 5-param. DDM	105	Static (21)	Static (21)	Static (21)	Static (21)	Static (21)	0.057	8811	9542

decreased again for the biggest time gaps (TTA of 7–8 s) leading to an inverted U-shaped RT-TTA-distribution. This inverted U-shape could represent participants making snap decisions based on initial distance: For short TTAs (where the initial distance from the car is smaller), they almost immediately decide to wait because the car is close; for long TTAs (where the car is further away), decision making is again rapid, as participants immediately judge the car as far away and quickly decide to cross. Consequently, if pedestrians decided to cross the road in front of the car they reacted faster if the car was driving at a higher speed (faster cars are further away given the same TTA — thereby creating an easier crossing decision). Conversely, if the decision was made to not cross the road, the decision was made faster if the car was going slowly (slower cars are closer given the same TTA — thereby creating an easier waiting decision).

3.2. Modelling

The condition-wise fitted 5-parameter DDM (Fig. 4) overall showed the best results in terms of goodness-of-fit (MSE) and partly also in model quality regarding simplicity (AIC), but narrowly lost to the Zgonnikov-DDM in BIC, due to the BIC placing a large penalty term for the number of parameters (see Table 1). The Zgonnikov-DDM scored best among the kinematics-dependent models in all indicators showing that the assumption of a dynamic drift rate and boundary separation can help improving the fit to our data. In terms of MSE, all condition-wise fitted models consistently showed better results in fitting the data than the kinematics-dependent models. Condition-wise models achieve this fit with a substantially larger number of parameters than kinematics-dependent models; when taking this fact into account by using the AIC as criterion, two models still outperformed the Zgonnikov-DDM, which is the best performing kinematics-dependent DDM: the condition-wise fitted 5-parameter DDM and the 4-parameter DDM with a Gaussian-distributed non-decision time. The reason why the AIC prefers these condition-wise fitted models over the Zgonnikov-DDM is that – although the penalty for the former having more parameters is about an order of magnitude larger than for the Zgonnikov-DDM – the penalty terms are small compared to the influence that the log likelihood (data | model) has on the AIC (where the condition-wise fitted models fit the data much better). On the other hand, only the best performing kinematics-dependent model, the Zgonnikov-DDM, outperformed the best condition-wise fitted DDM (the 5-parameter DDM)

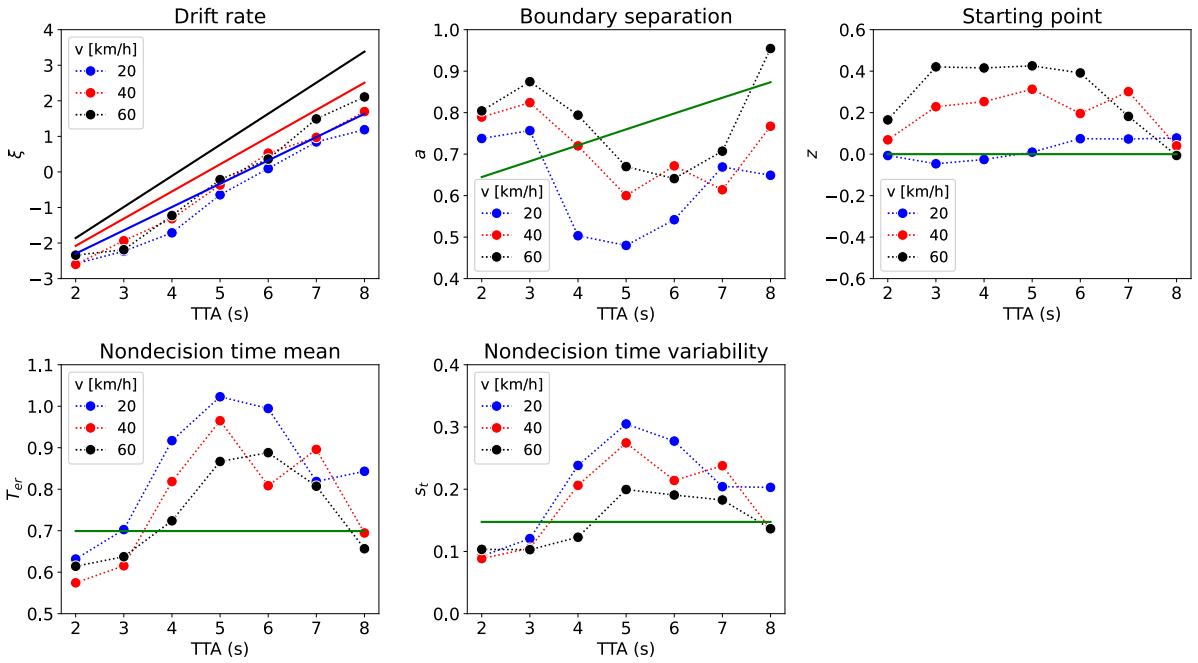

Fig. 4. Parameters of the condition-wise fitted 5-parameter DDM as the best-performing condition-wise fitted model (round markers) supplemented by the Zgonnikov-DDM as the best-performing kinematics-dependent model as a reference (solid lines). Coloured solid lines represent velocity-dependence, green solid lines represent velocity-independence. Dotted lines serve as a guide to the eye.

in terms of BIC, despite the large difference in estimated parameters between condition-wise fitted and kinematics-dependent models.

The condition-wise fitted 4-parameter DDM with a Gaussian-distributed non-decision time of variance s_t (Fig. 7 in Appendix A) scored the second best MSE and AIC value overall. We interpret that including an across-trial variability in the non-decision component of the reaction time is likely improving the overall fit, especially if the fitting is done per condition. According to Lerche and Voss (2016) including the intertrial variability of the non-decision time could counteract the negative influence of fast contaminants. The condition-wise fitted 5-parameter DDM is able to capture the kinematics-dependence (regarding TTA and speed) of the crossing probability as well as the reaction times for both decision outcomes (see Fig. 3). The model fits the choice and reaction time data well, however, reaction times are consistently predicted too small.

All condition-wise fitted drift-diffusion models show a monotonically increasing drift rate for larger time gaps (see Fig. 4, resp., Figs. 6, 7 and 8 in Appendix A). Additionally, the drift rate is higher the faster the approaching car is driving. Qualitatively, the drift rate in the condition-wise fitted models strongly resembles the assumed kinematics-dependency of the drift rate in the Giles- and Zgonnikov-DDMs (Fig. 4). This supports the assumption of a kinematics-dependent drift rate, that was made by previous pedestrian crossing decision-making studies (e.g., Markkula et al. (2018), Giles et al. (2019) and Pekkanen et al. (2022)), although not necessarily proving their exact functional form (e.g., assumed linearity).

Regarding the boundary, the results from the condition-wise fitted DDMs (see Fig. 4, resp., Figs. 6, 7 and 8 in Appendix A) do not fully resemble the assumed boundary from the Zgonnikov-DDM (see Figs 1(b) or 12) that is exponentially collapsing with smaller TTAs. Rather, we find a roughly U-shaped distribution with smallest boundary separation at medium TTAs of about 5 s and bigger separation towards smaller and bigger time gaps.

The fitting results of the 5-parameter DDM (see Fig. 4) for drift rates are remarkably similar regardless of vehicle speed. So, a lot of the speed-dependence seems to come from the starting point variations — which are quite big in relation to the boundary separation. This suggest a mechanism where pedestrians first look at the distance to the vehicle (which is here determined by a combination of TTA and speed) to form an initial idea of what decision to make and then they finalize that decision by looking at the TTA. For example, if the car is driving slowly (20 km/h) there is approximately no starting point bias ($z = 0$) for any time-gap. However, if the car is driving at medium (40 km/h) or high (60 km/h) speeds (which makes the vehicle spawn further away from the pedestrian), there is a proportional starting point bias towards the crossing option. Recent studies seem to support our results that a starting point bias proportional to the vehicle speed in the direction of the crossing decision improves the model fit (Zgonnikov et al., 2023). When we tried to restrict the starting point to non-positive values (representing a bias towards the waiting option) in additional model tests, the BIC results showed that model quality deteriorated dramatically. Regarding the distribution of non-decision time mean T_{er} and variability s_t in the condition-wise fitted 5-parameter DDM we each find an inverted U-shaped distribution regarding the TTA with a visible speed-dependency (higher non-decision time mean and variability for slower vehicles; see Fig. 4).

When comparing the condition-wise fitted 5-parameter DDM as the best-performing model overall to the Zgonnikov-DDM as the best-performing kinematics-dependent model, it is visible in Fig. 4 that in both models drift rates are monotonically increasing with TTA. However, drift rates are bigger (meaning more positive) in the Zgonnikov-DDM, compensating for the fact that positive starting biases were not allowed (unlike in the condition-wise fitted 5-parameter model).

Fig. 5 depicts the reaction time distributions (grey area) of crossing and waiting decisions for the different TTA (columns) and speed (rows) conditions. The black solid lines show the model fit of the condition-wise fitted 5-parameter DDM as the best-performing kinematics-dependent model and additionally as a reference the Zgonnikov-DDM (red dashed lines) as the best-performing kinematics-dependent model. For bigger time-gaps to the vehicle (within rows) the reaction time distributions are shifting more and more from waiting to crossing. For bigger velocities of the vehicle (within columns, so assuming constant time-gaps) the reaction time distributions are also shifting more and more from waiting to crossing (speed-dependency, e.g., Oxley et al. (2005)). Additionally, whereas the mode for crossing and waiting reaction times appear equal if the car drives at 20 km/h; for 40 km/h

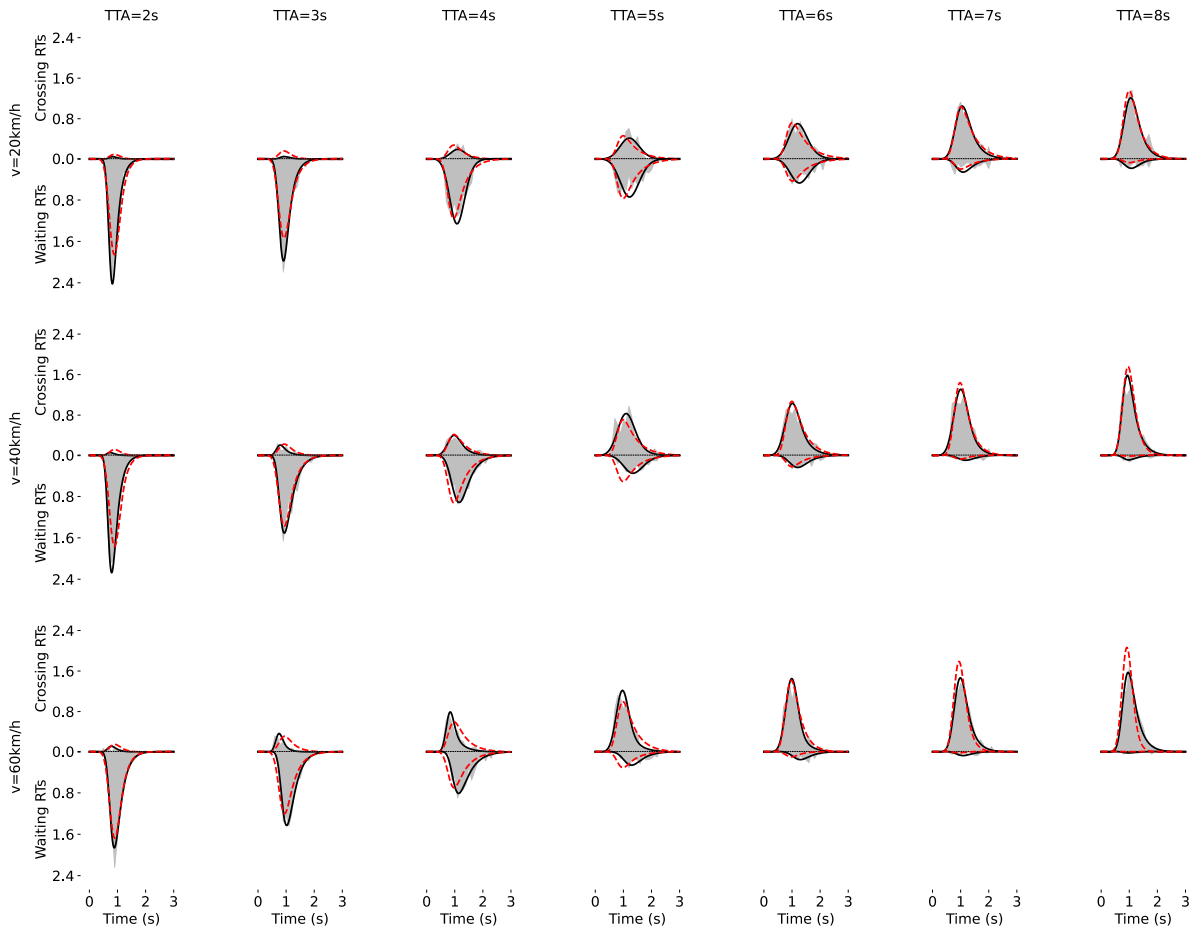

Fig. 5. Measured reaction time distributions (grey area) of crossing and waiting decisions for the different TTA (columns) and speed (rows) conditions; plus, model fits of the condition-wise fitted 5-parameter DDM (black solid lines) as the best-performing condition-wise fitted model and the Zgonnikov-DDM (red dashed lines) as the best-performing kinematics-dependent model.

and even more for 60 km/h the mode of the distributions are differing, namely crossing decisions happen faster than waiting decisions. The condition-wise fitted 5-parameter model is able to reproduce this asymmetry, whereas the Zgonnikov-model is not. This difference can be quantified with the help of Fig. 3 (right side), which shows that the condition-wise fitted 5-parameter model is better suited than the Zgonnikov-DDM to model the measured reaction time data. Furthermore, the Zgonnikov-DDM underestimates the maximum of waiting PDFs in most of the conditions, yet overestimates the maximum of crossing PDFs for conditions with high speed and high TTA (when the vehicle is far away). The condition-wise fitted 5-parameter model however is able to capture the form of the crossing and waiting PDFs better, making it the best model fit, also by visual inspection. Related to this point, the 5-parameter DDM is able to model the crossing probability for different vehicle TTAs and velocities quite accurately, whereas the kinematics-dependent Zgonnikov-DDM generally overestimates the pedestrians' crossing probability (compare Fig. 3, left side). With regard to these points, the kinematics-dependent models perform worse in terms of the goodness-of-fit. As a consequence, despite the reduced number of free parameters, the kinematics-dependent models also perform worse in AIC, but not in BIC. Overall, it is a close race between the model classes in BIC: first, third and fifth place are kinematics-dependent models, second and fourth place are fitted condition-wise. In other words, our AIC results suggest that the large number of parameters for the condition-wise fitted DDMs is warranted given the large improvement in goodness-of-fit, whereas our BIC results suggest the opposite, but by a smaller margin.

We checked for convergence of modelling results by decreasing the step size for numerically solving the Fokker–Planck equation (see Eq. (6) in Appendix A) by one order of magnitude ($dt = 0.001$ s), exemplary for the condition-wise fitted 5-parameter DDM. We found that all parameters (drift rate, boundary separation, starting point, non-decision time mean and variance) show similar values for all different TTA and velocity conditions. Also, MSE and BIC values were very similar. For this reason we assume that all initial calculations with $dt = 0.01$ s were valid (see Shinn et al. (2020) for reference).

Finally, we model all individuals in a Bayesian hierarchical model, making use of the dependency between individuals' data, to test whether our approach of pooling across participants led to any deviation in the estimation of DDM parameters. We performed additional hierarchical DDM calculations with the modelling framework HDDM (Wiecki et al., 2013). With the Bayesian hierarchical model, we find very similar trends for the estimated DDM parameters as in the non-hierarchical DDMs in our manuscript that neglect the inter-individual differences. Similar to the condition-wise fitted 3-parameter, 4-parameter and 5-parameter models, the drift rate is monotonically increasing with TTA from $\xi \approx -3$ for TTA = 2 s until $\xi \approx 2$ for TTA = 8 s with a flattening for very high TTAs (see Fig. 13 in Appendix A). For the boundary separation we similarly find a U-shaped distribution regarding TTA with the smallest boundary separation for TTA = 5 s as in the 5-parameter model (see Fig. 14 in Appendix A). The hierarchical fit also reproduces our initial findings for the condition-wise fitted 5-parameter DDM of a positive starting point bias that increases for smaller (time) gaps (see Fig. 15 in the Appendix A). Based on these results, we think that the validity of our original approach has been demonstrated.

4. Discussion

We compared two main classes of DDMs to model experimental pedestrian-crossing data, condition-wise fitted and kinematics-dependent DDMs. We find that the 5-parameter condition-wise fitted model provides a better goodness-of-fit (MSE) than any of the kinematics-dependent models. Importantly, the better model fit is not solely attributable of the former having more free parameters, as for overall model quality (AIC), which accounts of the number of parameters, the 5-parameter condition-wise fitted model also outperforms all other models tested, but not according to BIC. Summarizing these results, it is clear that the condition-wise fitted models fit the data much better than the kinematics-dependent models, which can be taken to indicate that there is clear room for further improvements to the exact formulations of current kinematics-dependent models. The AIC results are strongly in line with this perspective. The BIC results, with their larger penalty on model complexity, suggest that the very large improvements in goodness of fit may be due to excessive complexity of the condition-wise fitted models. This finding can be seen as a positive result for the general idea of kinematics-dependent models. Overall, we would argue that a reasonable conclusion from our findings is that there is substantial scope for improved formulations of kinematics-dependent models, but that these improved models should not need anywhere near as many parameters as the condition-wise fitted models we have tested here.

While in the field of human gap-acceptance decisions in traffic (e.g., pedestrians crossing roads (Giles et al., 2019; Pekkanen et al., 2022) or drivers performing left-turns with oncoming traffic (Zgonnikov et al., 2022, 2023)) kinematics-dependent DDMs are abundantly used, in other fields conventional (condition-wise fitted) DDMs are predominant. In our data the conventional models still show that there is a clear kinematics-dependency, which the condition-wise fitted DDMs do not model explicitly, but rather absorb it into a multitude of parameters. This suggests that there is room for further improvement for kinematics-based DDMs in pedestrian road crossing by obtaining a better understanding as to how the kinematics relates to decision variables.

All condition-wise fitted models support the assumption of a TTA-dependent and speed-dependent drift rate. The best-performing condition-wise fitted model (the 5-parameter DDM) showed that the introduction of a starting point bias could explain the speed-dependence of crossing decisions differently to previous research: At first pedestrians use the distance to the vehicle to form an initial idea of what decision to make. This distance-bias is modelled in the DDM by the starting point. This interpretation is consistent with the fact that the distance to the vehicle can in principle be inferred from a single instant (i.e., from a static picture), while speed and TTA estimates need integration of information over time. Hence, in contrast to speed or TTA, the distance to the vehicle can directly and immediately be derived at the start of the decision process. Only when the vehicle is approaching and its image is increasing on the observer's retina via visual looming (faster than a certain perceptual threshold) (Tian et al., 2022) pedestrians can use the TTA and integrate it into finalizing their decision regarding the road crossing.

In sum, there are various factors that influence pedestrian crossing decisions, which are not fully captured by standard DDM theory. One possible such difference is the dependence of drift rates on vehicle kinematics, as assumed by the Giles et al. (2019) and Zgonnikov et al. (2022) models. Another difference could be a rapid early evidence build-up from the initial view of how far away the car is. What we are doing in this paper is to fit standard DDMs condition-wise to probe what these underlying differences might be. The DDM drift rates we obtain support the hypothesis of kinematics-dependent (mostly TTA-dependent) drift rates, and the DDM starting points we obtain support this novel hypothesis of rapid early evidence build-up from the initial view of the vehicle distance. These results seem to be consistent with our interpretation that the initial distance of the vehicle leads pedestrians to prefer either crossing or waiting immediately at the onset of the trial. On the other hand, time is needed to integrate the additional information about how fast the vehicle is approaching into a TTA estimate and finalize the crossing decision. It will be an exciting issue for future studies to test a model that combines a TTA-dependent drift-rate and a distance-dependent starting point bias and to relate this to additional experimental data, but this is beyond the scope of this manuscript.

Regarding the boundary separation the results of the condition-wise fitted models indicate a small separation for medium time-gaps and a bigger separation for smaller but also bigger time-gaps. This contradicts earlier assumptions about specific kinematics-dependencies of decision boundaries, especially that of two symmetrically collapsing boundaries that was previously made to model gap acceptance in traffic (Zgonnikov et al., 2022). Recent studies on other traffic scenarios seem to support our findings that collapsing boundaries do not play a significant role in explaining human gap acceptance decisions in road traffic (Zgonnikov et al., 2023). One possible explanation could be the assumption of asymmetrical decision-bounds, for example, an exponentially collapsing waiting bound and an exponentially increasing crossing bound (similar to the kinematics-dependent model in Fig. 1(b), but with a crossing boundary horizontally mirrored at the half of the time axis). This specific boundary shape would also explain why crossing RTs are shorter than waiting RTs in our experiment: the longer one is accumulating evidence over time, the closer the car has approached in the meanwhile and therefore the more likely the waiting option becomes, while the crossing option gets more unlikely. Since there is currently no option to model asymmetric boundaries in PyDDM, this remains to be tested by future studies.

In general, one has to be careful in interpreting parameter values of the condition-wise fitted DDMs because different parameters can trade off against each other. For example, the dip in the middle for the boundary separation coincides with the peak in the middle for non-decision time (see Fig. 4), making those two potentially to some extend counteract each other (while having different individual effects on the joint distribution of reaction time and choice). So, whether it is just the model fit trying to capture a subtle aspect of the shape of the distribution and doing it by offsetting these parameters or whether it means something significant about the pedestrian's decision-making process is hard to differentiate. In summary, our results support the assumption of a drift rate that is monotonically increasing with TTA that was made by previous kinematics-dependent models (e.g., Markkula et al. (2018), Giles et al. (2019) and Pekkanen et al. (2022)), but not the assumption of (symmetrically) collapsing boundaries (e.g., Zgonnikov et al. (2022)) or an unbiased starting point for evidence accumulation (e.g., Markkula et al. (2018), Giles et al. (2019), Zgonnikov et al. (2022) and Pekkanen et al. (2022)) which is the reason why the condition-wise fitted models currently outperform the kinematics-dependent models according to MSE and AIC values.

Regarding the validity of our experimental approach, we consider it safe to assume that every participant is already very well trained in the gap-acceptance task prior to the experiment because of every day experience in road-traffic. Our experimental data shows that participants very rarely crossed at small TTAs, so we assume that it was uncomfortable to press the cross button when the vehicle was close (similar to a real-life scenario). To further prove the validity of our design we compared our results with reaction time data of other road crossing experiments. To our knowledge there is no other experiment that queries response times for the waiting decision nor response times in general in a real-traffic setting. There is, however, a VR cave study that reports the mean reaction time to a crossing opportunity of adults (indicated by pressing a button) to be 1.1 ± 0.1 s (Tapiro et al., 2020), which is very similar to our results of 1.11 ± 0.01 s for crossing and 1.13 ± 0.01 s for waiting, respectively.

When modelling or measuring road crossing, it is often assumed that pedestrians commence the crossing process after having come to a full stop. In this case, the decision to cross is clearly evident (by movement onset), while there is no obvious overt marker of the decision to wait. Consequently, most experimental studies (e.g., Lobjois et al. (2013), Zito et al. (2015) and Tapiro et al. (2016)) only query the timing of the crossing decision, and a non-response is considered a waiting decision, without any information about the latter's timing (go/no-go paradigm). We assume that pedestrians make a conscious decision in the real-world whether to cross or whether not-to-cross in front of an approaching vehicle. Hence we do not think that people in real-life make neither decision at all and just wait (completely undecided) until the car has passed. Therefore, we here decided to treat crossing and waiting decision more symmetrically and used a 2-afc paradigm, which is also the more commonly used approach for testing DDMs in a wide range of contexts. Importantly, key findings of go/no-go pedestrian crossing tasks – most relevantly, the speed-dependence of gap acceptance – are replicated in our 2-afc paradigm, making it unlikely that the report mode influences the decision as such. Consequently, the 2-afc task has the advantage to provide substantial additional information (the distribution of decision times for waiting), which allow us a more detailed model comparison.

In addition, the presumption that road crossing starts from a stationary situation might not hold generally for real-life situations (Gorrini et al., 2018), such that there are also overt signals of the waiting decision (slowing down or stopping). It will be an interesting issue for further research to experimentally test road crossing behaviour for pedestrians approaching the curb walking, for example by combining virtual reality with motion capture. Such a setting would also allow capturing more than the one-dimensional decision available from a button press, as in reality, the decision may be signalled by a high-dimensional set of parameters (walking speed, trajectory, posture, angle between joints etc.; Kalantarov et al. (2017)). Nonetheless, in the end a decision has to be reached and to obtain meaningful data from high-dimensional data, they need to be reduced in a meaningful way, which again can be aided by appropriate behavioural models developed using paradigms and scenarios of reduced complexity. This has also been our rationale to start with a scenario that includes only one car and one pedestrian, but extending DDMs to cover situations with more cars will be an exciting prospect for further experimental and modelling research.

In traffic, humans typically obtain good predictions of other road users' behaviour. For pedestrians with respect to cars this is a skill that needs to be acquired during childhood (Tapiro et al., 2016; Biassoni et al., 2018), and in turn, drivers need to be able to estimate pedestrian behaviour. The fact that this is done while occupied with other driving related tasks, suggests that human drivers in most cases accomplish the reduction of the high-dimensional data available when sighting a pedestrian at the curbside to a robust estimate of their crossing intention with ease, while this is still a major challenge for autonomous vehicles (Kooij et al., 2014). Hence, computational cognitive models, like investigated herein, are a key step towards and beyond human-like performance for such systems (Janssen et al., 2022). A sound understanding of human behaviour and its formalization in cognitive models will aid the development of automated vehicles in at least three respects: (i) The prediction of VRU's (e.g., pedestrian's) behaviour is improved. (ii) The automated vehicle can adapt its own driving choices to be more human-like and thereby signal its intentions towards human road users in an unambiguous and readily accessible way. This also increases the vehicle's ability to nudge humans to make decisions (Zgonnikov et al., 2023), for example, encouraging pedestrians to cross the road by slowing down briefly when approaching. (iii) Unlike self-learning algorithms, for which explainability is a challenge (Gunning and Aha, 2019), decision variables in cognitive models are typically readily interpretable. This makes it easier to assign responsibility and consequently liability (e.g., in case of an accident) and therefore may help overcoming legal and acceptance challenges that may impede the wide-spread deployment of autonomous vehicles. Hence, the development of autonomous vehicles will benefit from good and experimentally-validated cognitive models that approximate the human decision process, towards which we here present a relevant stepping stone.

CRediT authorship contribution statement

Max Theisen: Conceptualization, Data curation, Formal analysis, Investigation, Methodology, Software, Validation, Visualization, Writing – original draft. **Caroline Schießl:** Conceptualization, Funding acquisition, Supervision, Writing – review & editing. **Wolfgang Einhäuser:** Conceptualization, Funding acquisition, Supervision, Writing – review & editing. **Gustav Markkula:** Conceptualization, Supervision, Writing – review & editing, Funding acquisition.

Declaration of competing interest

The authors declare that they have no known competing financial interests or personal relationships that could have appeared to influence the work reported in this paper.

Data availability

Data will be made available on request.

Acknowledgements

Max Theisen and Caroline Schießl received support from the Japanese-German Research Collaboration on Human Factors in Connected and Automated Driving (CADJapanGermany) that was supported by the German Federal Ministry of Education and Research (funding code 16ES1038). Wolfgang Einhäuser received support from Deutsche Forschungsgemeinschaft (DFG, German Research Foundation) project ID 416228727. Gustav Markkula received support from the UK Engineering and Physical Sciences Research Council, grant agreement EP/S005056/1. We kindly thank our colleague Matthias Beggiato from Chemnitz University of Technology, who provided a jsPsych code template for the experimental part of this study.

Appendix A

Modelling details

The accumulated evidence x in the drift-diffusion model can be expressed mathematically with a differential equation:

$$dx = \xi(x,t)dt + \sigma(x,t)dW \tag{5}$$

with the drift $\xi(x,t)$ and the diffusion coefficient $D(x,t) = \sigma^2(x,t)/2$ of the Wiener process W. To analyse the participants' decision-making, we used the drift-diffusion modelling framework PyDDM (see details in Shinn et al. (2020)), which numerically solves the DDM equation (5) using the Fokker–Planck equation (6):

$$\frac{\partial}{\partial t}p(x,t) = -\frac{\partial}{\partial x}\left[\xi(x,t)p(x,t)\right] + \frac{\partial^2}{\partial x^2}\left[D(x,t)p(x,t)\right] \tag{6}$$

The Fokker–Planck equation describes the time evolution of the probability density function $p(x,t)$ under the influence of drift and diffusion. We employed maximum likelihood estimation as the fitting method to estimate the parameters of the drift-diffusion-model. We fitted by using the full-distribution maximum likelihood on the full probability distribution (Shinn et al., 2020). The optimization algorithm used in the fitting process was differential evolution (Storn and Price, 1997). The models were simulated for a duration of $T_{dur} = 3$ s with a reasonable (Shinn et al., 2020) time-step of $dt = 0.01$ s and an evidence grid size of $dx = 0.001$. For an introduction to the logic and structure of evidence accumulation models and DDMs, see for example Ratcliff et al. (2016) and Dutilh et al. (2019).

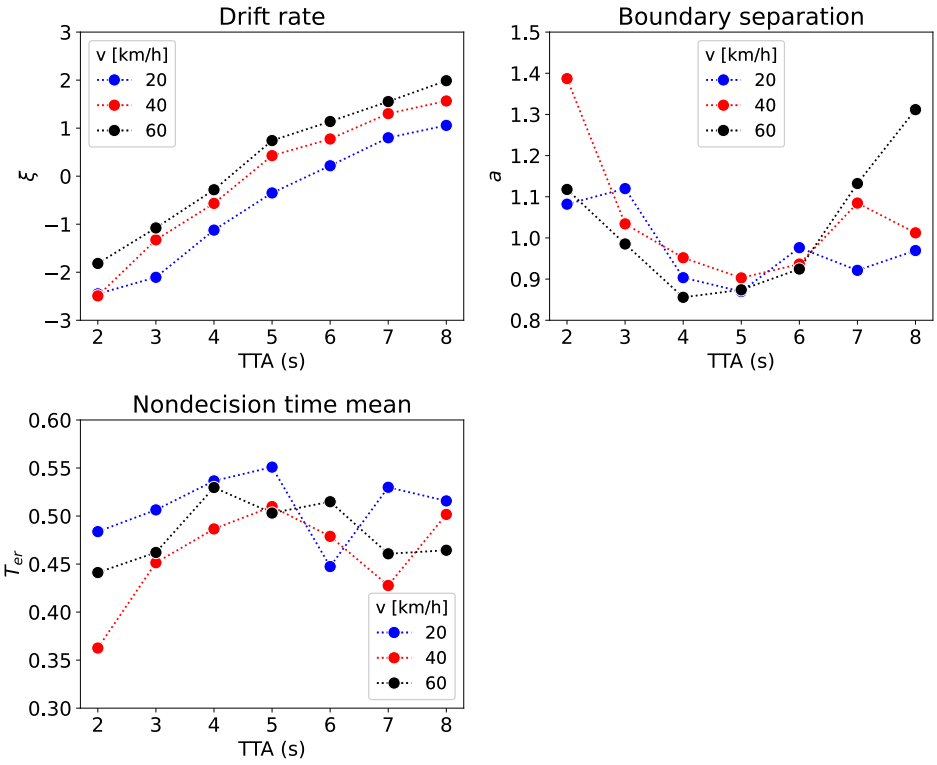

Fig. 6. Parameters of the condition-wise fitted 3-parameter DDM. Per TTA- and velocity-condition a separate model was fitted. Data was aggregated over all participants. Dotted lines serve as a guide to the eye.

Table 2
Model parameter values of the condition-wise fitted 3-parameter DDM.

v (km/h)	TTA (s)	Drift rate	Boundary separation	Non-decision time mean
20	2	−2.45059117	1.08198777	0.48378354
20	3	−2.10599752	1.11979932	0.50640773
20	4	−1.12299546	0.9034387	0.53658031
20	5	−0.34914691	0.86978613	0.55092393
20	6	0.2169275	0.97636514	0.44741754
20	7	0.79967791	0.9212585	0.52994509
20	8	1.05752427	0.96938403	0.5157492
40	2	−2.49251848	1.38692817	0.3625686
40	3	−1.32567163	1.03411283	0.45143325
40	4	−0.56682339	0.95182208	0.48657254
40	5	0.4274359	0.90291679	0.50984859
40	6	0.77401328	0.93652023	0.47885267
40	7	1.30265647	1.0846644	0.42770143
40	8	1.56583106	1.01234381	0.50169025
60	2	−1.81733776	1.11774067	0.44116137
60	3	−1.07740981	0.98529717	0.46208506
60	4	−0.28260581	0.85570412	0.5296974
60	5	0.74141644	0.87396725	0.50311926
60	6	1.13837	0.92440629	0.5149182
60	7	1.55373188	1.13212721	0.46069674
60	8	1.98785005	1.31164788	0.46438048

3-parameter DDM

See Fig. 6 and Table 2.

4-parameter DDM (ND-time variance)

See Fig. 7 and Table 3.

4-parameter DDM (starting point)

See Fig. 8 and Table 4.

5-parameter DDM

See Fig. 9 and Table 5.

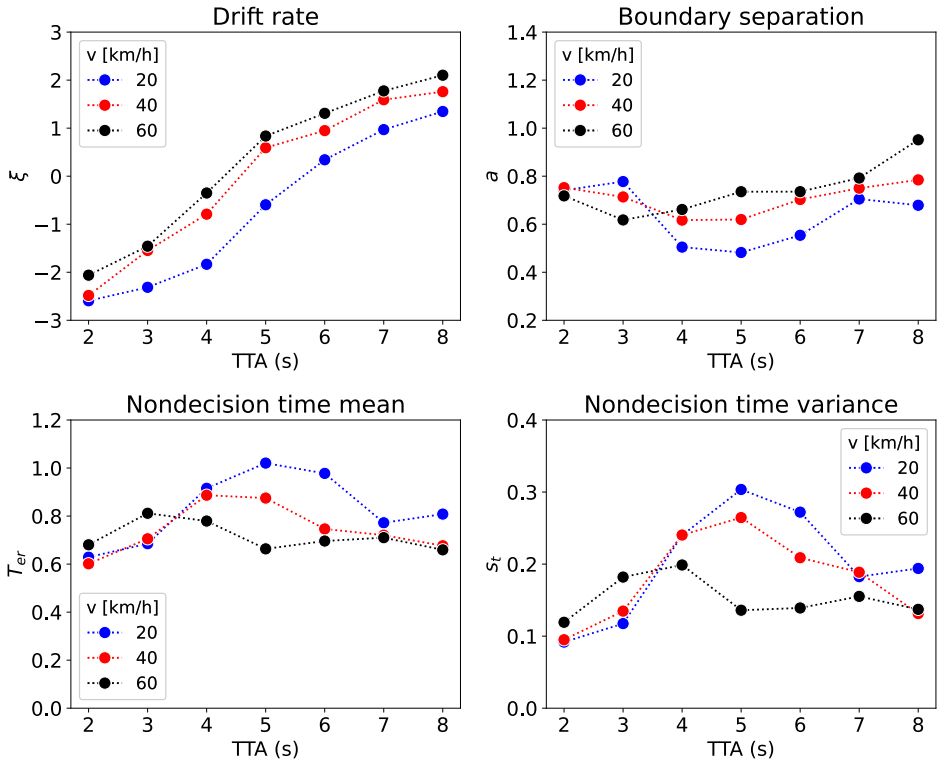

Fig. 7. Parameters of the cond.-wise fitted 4-parameter DDM (ND-time variance). Per TTA- and velocity-condition a separate model was fitted. Data was aggregated over all participants. Dotted lines serve as a guide to the eye.

Table 3
Model parameter values of the condition-wise fitted 4-parameter DDM (ND-time variance).

v (km/h)	TTA (s)	Drift rate	Boundary separation	Non-decision time mean	Non-decision time variance
20	2	−2.59395623	0.74122869	0.62905132	0.09179156
20	3	−2.31346934	0.77758017	0.68500675	0.11744086
20	4	−1.83421976	0.50470235	0.91563532	0.24000972
20	5	−0.59518924	0.48222954	1.02066815	0.303595
20	6	0.3413216	0.5538931	0.97766569	0.27212553
20	7	0.96967901	0.7050376	0.77215506	0.18259652
20	8	1.34683099	0.67891883	0.8082147	0.19398363
40	2	−2.48283049	0.75232177	0.6014223	0.0950447
40	3	−1.54724238	0.71355475	0.70545399	0.1347646
40	4	−0.79094058	0.61707321	0.88688655	0.24038507
40	5	0.59265367	0.61961943	0.87501502	0.26460143
40	6	0.94886711	0.70290233	0.74640145	0.20884285
40	7	1.59170442	0.75002801	0.72038353	0.18869439
40	8	1.75952649	0.78467845	0.67645048	0.13134068
60	2	−2.06105913	0.71804797	0.68047172	0.11926084
60	3	−1.45793227	0.61775599	0.81166474	0.18200871
60	4	−0.35021807	0.66137457	0.77932642	0.19878185
60	5	0.83597855	0.73535709	0.66353104	0.13598394
60	6	1.30875138	0.7355759	0.69614105	0.13912023
60	7	1.77544956	0.79231134	0.71016069	0.1552216
60	8	2.10225199	0.95149109	0.65942804	0.13719726

Ratcliff-DDM in Zgonnikov et al. (2022)

See Fig. 10 and Table 6.

Giles-DDM in Zgonnikov et al. (2022)

See Fig. 11 and Table 7.

Zgonnikov-DDM in Zgonnikov et al. (2022)

See Fig. 12 and Table 8.

Bayesian hierarchical model

See Figs. 13–15.

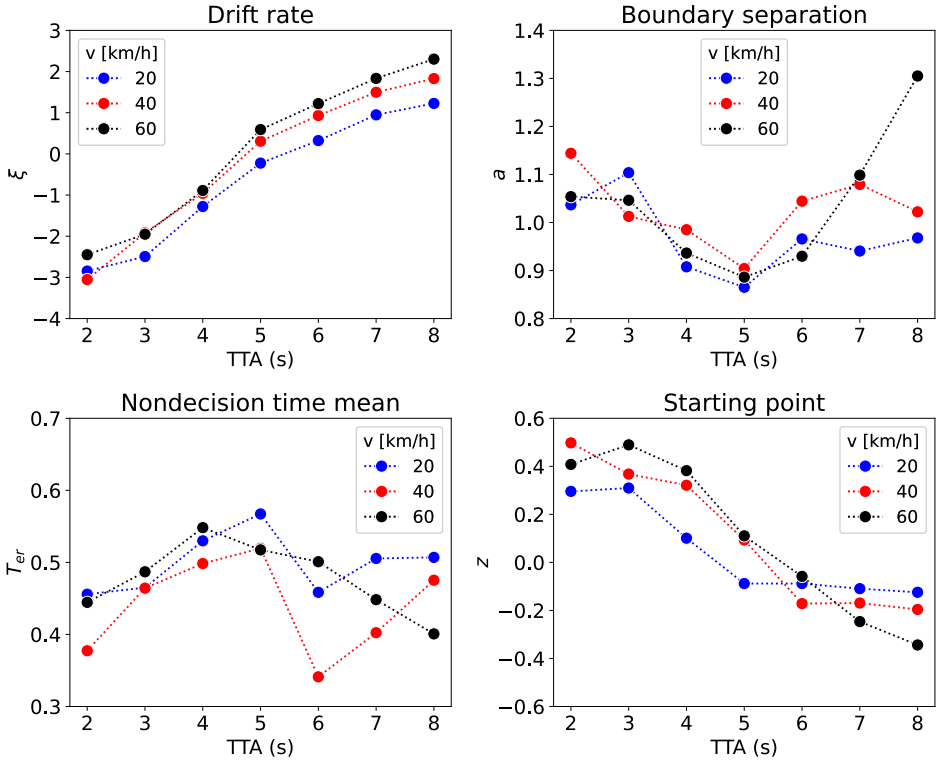

Fig. 8. Parameters of the condition-wise fitted 4-parameter DDM (Starting point). Per TTA- and velocity-condition a separate model was fitted. Data was aggregated over all participants. Dotted lines serve as a guide to the eye.

Table 4
Model parameter values of the condition-wise fitted 4-parameter DDM (Starting point).

v (km/h)	TTA (s)	Drift rate	Boundary separation	Starting point	Non-decision time mean
20	2	−2.84647845	1.03675559	0.29571416	0.45582907
20	3	−2.49375458	1.10375226	0.30968731	0.46501535
20	4	−1.2787609	0.90770831	0.10077709	0.5299224
20	5	−0.22436691	0.86514477	−0.08807932	0.56723196
20	6	0.32305085	0.96577246	−0.08813005	0.4584566
20	7	0.94809042	0.94058536	−0.10934114	0.50544489
20	8	1.22599861	0.96787135	−0.12457563	0.50699677
40	2	−3.05256529	1.14414367	0.49762994	0.37738377
40	3	−1.91772823	1.01274862	0.36775062	0.46423681
40	4	−0.95799431	0.98504631	0.32119519	0.498403
40	5	0.30701618	0.9041317	0.093336	0.51952436
40	6	0.93127309	1.04439983	−0.17159335	0.3411488
40	7	1.49702285	1.07930748	−0.16922413	0.40237351
40	8	1.82898616	1.0222041	−0.19607891	0.47526085
60	2	−2.44900356	1.05387427	0.40795847	0.44451329
60	3	−1.951104	1.04631719	0.48944321	0.48696021
60	4	−0.88920847	0.93637193	0.38206275	0.54825235
60	5	0.59047126	0.88629378	0.11043719	0.51738357
60	6	1.22073968	0.92980789	−0.058365	0.50092546
60	7	1.83344955	1.09861291	−0.24651016	0.44827616
60	8	2.30188125	1.30499999	−0.3438489	0.40075279

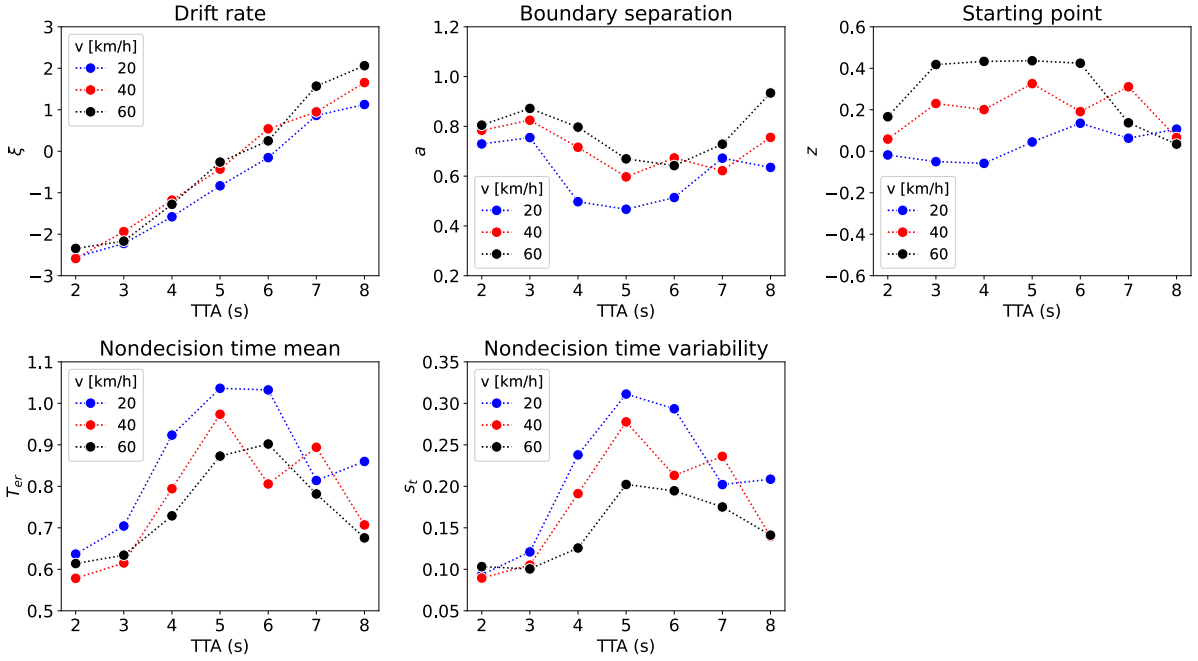

Fig. 9. Parameters of the condition-wise fitted 5-parameter DDM. Per TTA- and velocity-condition a separate model was fitted. Data was aggregated over all participants. Dotted lines serve as a guide to the eye.

Table 5
Model parameter values of the condition-wise fitted 5-parameter DDM.

v (km/h)	TTA (s)	Drift rate	Boundary separation	Starting point	Non-decision time mean	Non-decision time variance
20	2	−2.52654139	0.72385446	−0.03507681	0.64218557	0.09469506
20	3	−2.16560848	0.74103367	−0.08114234	0.71662348	0.12334117
20	4	−1.55192445	0.49546691	−0.06539154	0.92534196	0.23809625
20	5	−0.64633761	0.47872858	0.00972628	1.02404378	0.30529462
20	6	−0.20682009	0.497	0.13954743	1.04957384	0.30099839
20	7	0.93692338	0.69499933	0.01975445	0.78479569	0.18844778
20	8	1.15416523	0.6415575	0.09367803	0.85217766	0.20588482
40	2	−2.60380434	0.79044789	0.07114518	0.57363577	0.08837145
40	3	−1.89553453	0.81578827	0.20733488	0.62095519	0.10576159
40	4	−1.315039	0.728	0.25906828	0.79314809	0.19362861
40	5	−0.77704634	0.58600008	0.3813472	1.0141443	0.29415281
40	6	0.41453556	0.659	0.24209529	0.83375585	0.22286647
40	7	1.02243264	0.63202608	0.28551786	0.87755512	0.23080014
40	8	1.64854127	0.75383088	0.07026277	0.70895204	0.14003594
60	2	−2.28933158	0.7834927	0.1378943	0.62660392	0.10869637
60	3	−2.16109466	0.84565634	0.40487448	0.64957596	0.10600535
60	4	−1.30826107	0.81028997	0.44557951	0.72283876	0.11611412
60	5	−0.16361374	0.67099998	0.41280883	0.85876734	0.19598005
60	6	0.27366551	0.64309618	0.41888455	0.8989531	0.1935539
60	7	1.58317349	0.73199999	0.12908308	0.77733222	0.17388544
60	8	2.11013325	0.95508304	−0.00683118	0.65610238	0.13640722

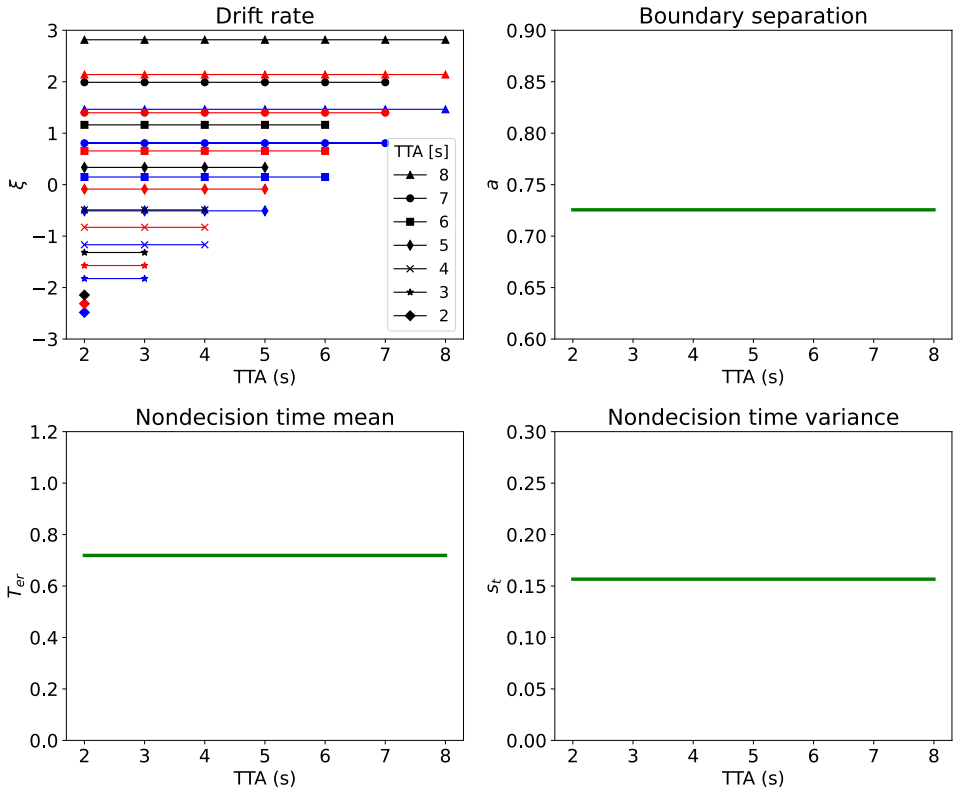

Fig. 10. Parameters of the kinematics-dependent Ratcliff-DDM in Zgonnikov et al. (2022) adapted after Ratcliff (1978). A single model was fitted over all TTA- and velocity-conditions. Data was aggregated over all participants. Drift rates are static over time per condition and depend on speed and TTA of the approaching vehicle at the start of the trial. Colour-coding is blue for 20 km/h, red for 40 km/h and black for 60 km/h. Boundary separation, non-decision time mean and variance are constant over time for all TTAs and velocities of the car.

Table 6
Model parameter values of the kinematics-dependent Ratcliff-DDM.

v (km/h)	TTA (s)	Drift rate	Boundary separation	Non-decision time mean	Non-decision time variance
20	2	−2.48283145	0.725539	0.718868	0.156660
20	3	−1.8250082	”	”	”
20	4	−1.1671850	”	”	”
20	5	−0.5093618	”	”	”
20	6	0.14846130	”	”	”
20	7	0.80628449	”	”	”
20	8	1.46410768	”	”	”
40	2	−2.3139010	”	”	”
40	3	−1.5716126	”	”	”
40	4	−0.8293243	”	”	”
40	5	−0.0870359	”	”	”
40	6	0.65525244	”	”	”
40	7	1.39754082	”	”	”
40	8	2.13982920	”	”	”
60	2	−2.1449706	”	”	”
60	3	−1.3182171	”	”	”
60	4	−0.4914635	”	”	”
60	5	0.33529001	”	”	”
60	6	1.16204357	”	”	”
60	7	1.98879714	”	”	”
60	8	2.81555071	”	”	”

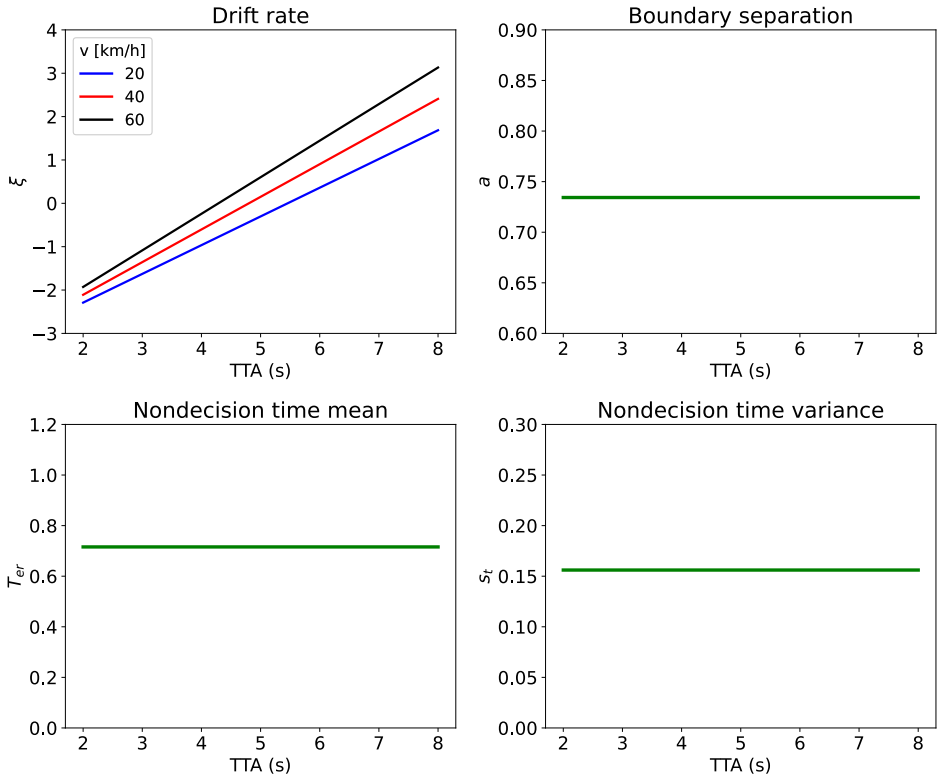

Fig. 11. Parameters of the kinematics-dependent Giles-DDM in Zgonnikov et al. (2022) adapted after Giles et al. (2019). A single model was fitted over all TTA- and velocity-conditions. Data was aggregated over all participants. Boundary separation, non-decision time mean and variance are constant over time for all TTAs and velocities of the car.

Table 7
Model parameter values of the kinematics-dependent Giles-DDM.

v (km/h)	TTA (s)	Drift rate	Boundary separation	Non-decision time mean	Non-decision time variance
20	2	−2.29040825	0.734311	0.715728	0.156082
20	3	−1.62781225	”	”	”
20	4	−0.96521626	”	”	”
20	5	−0.30262026	”	”	”
20	6	0.35997574	”	”	”
20	7	1.02257173	”	”	”
20	8	1.68516773	”	”	”
40	2	−2.10957426	”	”	”
40	3	−1.35656126	”	”	”
40	4	−0.60354827	”	”	”
40	5	0.14946473	”	”	”
40	6	0.90247772	”	”	”
40	7	1.65549071	”	”	”
40	8	2.40850371	”	”	”
60	2	−1.92874026	”	”	”
60	3	−1.08531027	”	”	”
60	4	−0.24188028	”	”	”
60	5	0.60154971	”	”	”
60	6	1.4449797	”	”	”
60	7	2.28840969	”	”	”
60	8	3.13183968	”	”	”

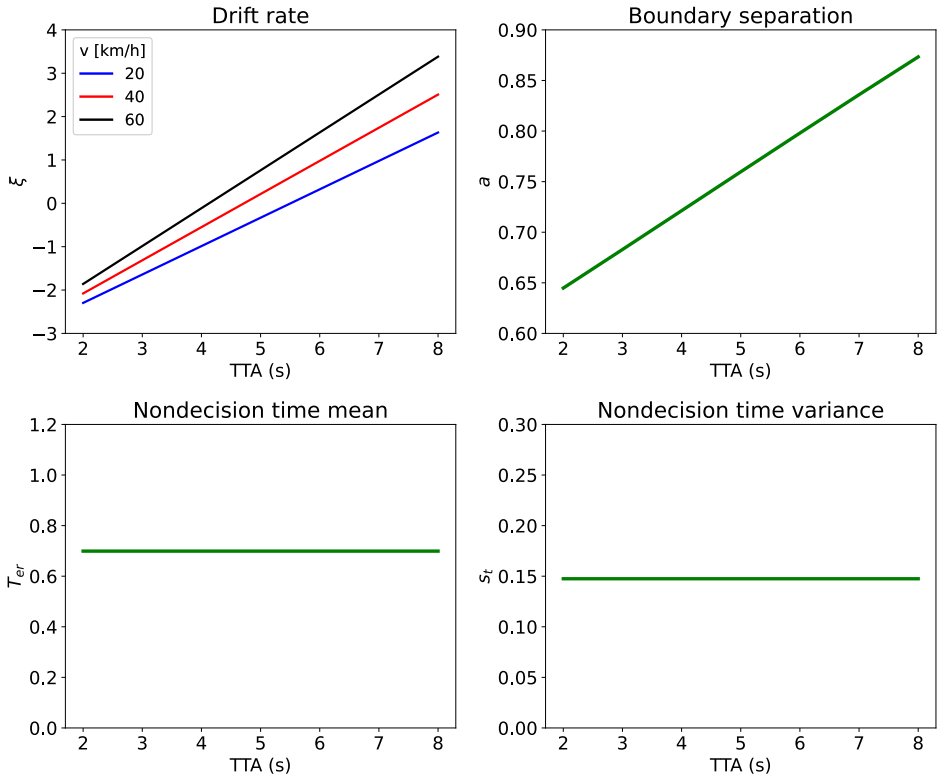

Fig. 12. Parameters of the kinematics-dependent Zgonnikov-DDM in Zgonnikov et al. (2022). A single model was fitted over all TTA- and velocity-conditions. Data was aggregated over all participants. Boundary separation is exponentially decreasing for smaller TTAs independent of the vehicle's velocity. Non-decision time mean and variance are constant over time for all TTAs and velocities of the car.

Table 8
Model parameter values of the kinematics-dependent Zgonnikov-DDM.

v (km/h)	TTA (s)	Drift rate	Boundary separation	Non-decision time mean	Non-decision time variance
20	2	−2.29735775	0.64479673	0.699153	0.147472
20	3	−1.64231754	0.68289979	”	”
20	4	−0.98727732	0.7212748	”	”
20	5	−0.33223711	0.75971197	”	”
20	6	0.3228031	0.79800012	”	”
20	7	0.97784331	0.83593134	”	”
20	8	1.63288353	0.87330544	”	”
40	2	−2.07865732	0.64479673	”	”
40	3	−1.3142669	0.68289979	”	”
40	4	−0.54987647	0.7212748	”	”
40	5	0.21451395	0.75971197	”	”
40	6	0.97890438	0.79800012	”	”
40	7	1.7432948	0.83593134	”	”
40	8	2.50768523	0.87330544	”	”
60	2	−1.8599569	0.64479673	”	”
60	3	−0.98621626	0.68289979	”	”
60	4	−0.11247562	0.7212748	”	”
60	5	0.76126502	0.75971197	”	”
60	6	1.63500565	0.79800012	”	”
60	7	2.50874629	0.83593134	”	”
60	8	3.38248693	0.87330544	”	”

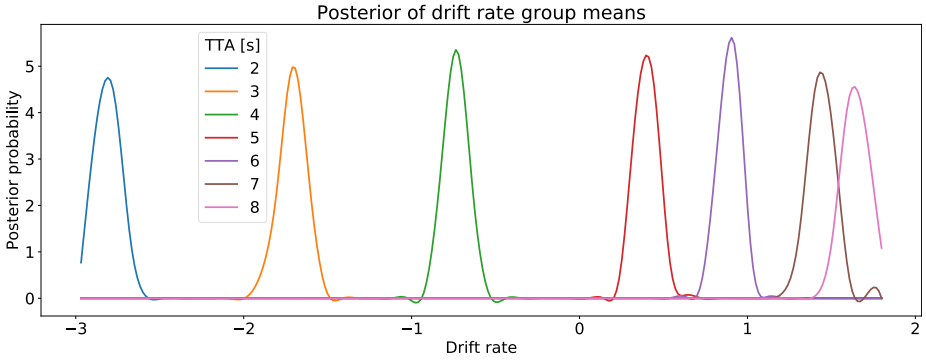

Fig. 13. Posterior probabilities for different drift rates ξ for each TTA condition merged over all velocity conditions.

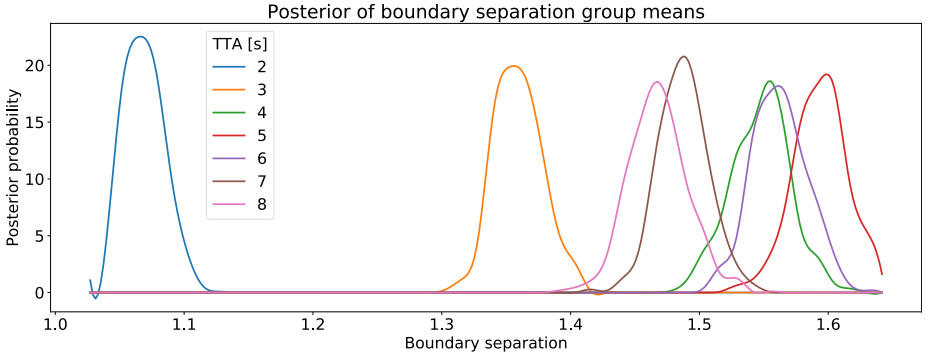

Fig. 14. Posterior probabilities for different boundary separations a for each TTA condition merged over all velocity conditions.

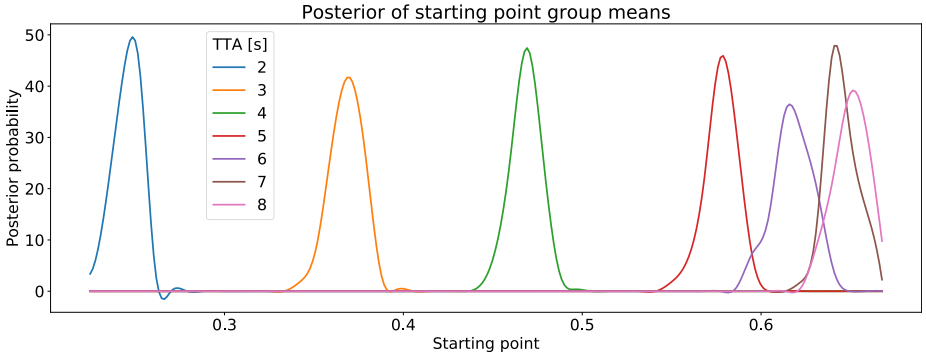

Fig. 15. Posterior probabilities for different starting points z for each TTA condition merged over all velocity conditions.

Appendix B. Supplementary data

Supplementary material related to this article can be found online at https://doi.org/10.1016/j.ijhcs.2023.103200.

References

Biassoni, F., Bina, M., Confalonieri, F., Ciceri, M., 2018. Visual exploration of pedestrian crossings by adults and children: Comparison of strategies. Transp. Res. F 56, https://doi.org/10.1016/j.trf.2018.04.009.

Bridges, D., Pitiot, A., MacAskill, M., Peirce, J., 2020. The timing mega-study: comparing a range of experiment generators, both lab-based and online. PeerJ 8, e9414, https://doi.org/10.7717/peerj.9414.

De Leeuw, J.R., 2015. jsPsych: A JavaScript library for creating behavioral experiments in a web browser. Behav. Res. Methods 47 (1), 1–12, https://doi.org/10.3758/s13428-014-0458-y.

Dosovitskiy, A., Ros, G., Codevilla, F., Lopez, A., Koltun, V., 2017. CARLA: An open urban driving simulator. In: Conference on Robot Learning. PMLR, pp. 1–16, https://doi.org/10.48550/arXiv.1711.03938.

Dutilh, G., Annis, J., Brown, S.D., Cassey, P., Evans, N.J., Grasman, R.P., Hawkins, G.E., Heathcote, A., Holmes, W.R., Krypotos, A.-M., et al., 2019. The quality of response time data inference: A blinded, collaborative assessment of the validity of cognitive models. Psychon. Bull. Rev. 26, 1051–1069, https://doi.org/10.3758/s13423-017-1417-2.

Farrell, S., Lewandowsky, S., 2018. Computational Modeling of Cognition and Behavior. Cambridge University Press, pp. 369–386.
Giles, O., Markkula, G., Pekkanen, J., Yokota, N., Matsunaga, N., Merat, N., Daimon, T., 2019. At the zebra crossing: Modelling complex decision processes with variable-drift diffusion models. In: Proceedings of the 41st Annual Meeting of the Cognitive Science Society. Cognitive Science Society, pp. 366–372, https://doi.org/10.31234/osf.io/cgj7r.
Gorrini, A., Crociani, L., Vizzari, G., Bandini, S., 2018. Observation results on pedestrian-vehicle interactions at non-signalized intersections towards simulation. Transp. Res. F 59, 269–285, https://doi.org/10.1016/j.trf.2018.09.016.
Gunning, D., Aha, D., 2019. Darpa's explainable artificial intelligence (XAI) program. AI Mag. 40 (2), 44–58.
Hubert, M., Vandervieren, E., 2008. An adjusted boxplot for skewed distributions. Comput. Statist. Data Anal. 52 (12), 5186–5201, https://doi.org/10.1016/j.csda.2007.11.008.
Janssen, C.P., Baumann, M., Oulasvirta, A., Iqbal, S.T., Heinrich, L., 2022. Computational models of human-automated vehicle interaction (dagstuhl seminar 22102). In: Dagstuhl Reports, Vol. 12. (3), Schloss Dagstuhl-Leibniz-Zentrum für Informatik, https://doi.org/10.4230/DagRep.12.3.15.
Kalantarov, S., Riemer, R., Oron-Gilad, T., 2017. Pedestrians' road crossing decisions and body parts' movements. Transp. Res. F 53, 155–171, https://doi.org/10.1016/j.trf.2017.09.012.
Kooij, J.F.P., Schneider, N., Flohr, F., Gavrila, D.M., 2014. Context-based pedestrian path prediction. In: European Conference on Computer Vision. Springer, pp. 618–633, https://doi.org/10.1007/978-3-319-10599-4_40.
Lerche, V., Voss, A., 2016. Model complexity in diffusion modeling: Benefits of making the model more parsimonious. Front. Psychol. 7, 1324, https://doi.org/10.3389/fpsyg.2016.01324.
Lerche, V., Voss, A., Nagler, M., 2017. How many trials are required for parameter estimation in diffusion modeling? A comparison of different optimization criteria. Behav. Res. Methods 49, 513–537, https://doi.org/10.3758/s13428-016-0740-2.
Li, L., Ota, K., Dong, M., 2018. Humanlike driving: Empirical decision-making system for autonomous vehicles. IEEE Trans. Veh. Technol. 67 (8), 6814–6823, https://doi.org/10.1109/TVT.2018.2822762.
Litman, T., 2013. Autonomous Vehicle Implementation Predictions. Technical Report, Victoria Transport Policy Institute.
Litman, T., 2022. Autonomous Vehicle Implementation Predictions. Technical Report, Victoria Transport Policy Institute.
Lobjois, R., Benguigui, N., Cavallo, V., 2013. The effects of age and traffic density on street-crossing behavior. Accid. Anal. Prev. 53, 166–175, https://doi.org/10.1016/j.aap.2012.12.028.
Lobjois, R., Cavallo, V., 2007. Age-related differences in street-crossing decisions: The effects of vehicle speed and time constraints on gap selection in an estimation task. Accid. Anal. Prev. 39 (5), 934–943, https://doi.org/10.1016/j.aap.2006.12.013.
Luu, D., 2017. Keyboard latency. https://danluu.com/keyboard-latency/. Retrieved on: 2022-08-10.
Markkula, G., Dogar, M.R., 2022. Models of human behavior for human-robot interaction and automated driving: How accurate do the models of human behavior need to be? IEEE Robot. Autom. Mag. 2–7, https://doi.org/10.1109/MRA.2022.3182892.
Markkula, G., Romano, R., Madigan, R., Fox, C.W., Giles, O.T., Merat, N., 2018. Models of human decision-making as tools for estimating and optimizing impacts of vehicle automation. Transp. Res. Rec. 2672 (37), 153–163, https://doi.org/10.1177/0361198118792131.
Oxley, J.A., Ihsen, E., Fildes, B.N., Charlton, J.L., Day, R.H., 2005. Crossing roads safely: an experimental study of age differences in gap selection by pedestrians. Accid. Anal. Prev. 37 (5), 962–971, https://doi.org/10.1016/j.aap.2005.04.017.
Pekkanen, J., Giles, O.T., Lee, Y.M., Madigan, R., Daimon, T., Merat, N., Markkula, G., 2022. Variable-drift diffusion models of pedestrian road-crossing decisions. Comput. Brain Behav. 5 (1), 60–80, https://doi.org/10.1007/s42113-021-00116-z.
Petzoldt, T., 2014. On the relationship between pedestrian gap acceptance and time to arrival estimates. Accid. Anal. Prev. 72, 127–133, https://doi.org/10.1016/j.aap.2014.06.019.
Rasouli, A., Tsotsos, J.K., 2019. Autonomous vehicles that interact with pedestrians: A survey of theory and practice. IEEE Trans. Intell. Transp. Syst. 21 (3), 900–918, https://doi.org/10.1109/TITS.2019.2901817.
Ratcliff, R., 1978. A theory of memory retrieval. Psychol. Rev. 85 (2), 59, https://doi.org/10.1037/0033-295X.85.2.59.
Ratcliff, R., McKoon, G., 2008. The diffusion decision model: theory and data for two-choice decision tasks. Neural Comput. 20 (4), 873–922, https://doi.org/10.1162/neco.2008.12-06-420.
Ratcliff, R., Rouder, J.N., 1998. Modeling response times for two-choice decisions. Psychol. Sci. 9 (5), 347–356, https://doi.org/10.1111/1467-9280.00067.
Ratcliff, R., Smith, P.L., Brown, S.D., McKoon, G., 2016. Diffusion decision model: Current issues and history. Trends Cogn. Sci. 20 (4), 260–281, https://doi.org/10.1016/j.tics.2016.01.007.
Ratcliff, R., Tuerlinckx, F., 2002. Estimating parameters of the diffusion model: Approaches to dealing with contaminant reaction times and parameter variability. Psychon. Bull. Rev. 9 (3), 438–481, https://doi.org/10.3758/BF03196302.
Schmidt, S., Faerber, B., 2009. Pedestrians at the kerb–recognising the action intentions of humans. Transp. Res. F 12 (4), 300–310, https://doi.org/10.1016/j.trf.2009.02.003.
Schwall, M., Daniel, T., Victor, T., Favaro, F., Hohnhold, H., 2020. Waymo public road safety performance data. arXiv. http://dx.doi.org/10.48550/arXiv.2011.00038.
Schwarting, W., Alonso-Mora, J., Rus, D., 2018. Planning and decision-making for autonomous vehicles. Annu. Rev. Control Robot. Auton. Syst. 1, 187–210, https://doi.org/10.1146/annurev-control-060117-105157.
Shinn, M., Lam, N.H., Murray, J.D., 2020. A flexible framework for simulating and fitting generalized drift-diffusion models. eLife 9, e56938, https://doi.org/10.7554/eLife.56938.
Storn, R., Price, K., 1997. Differential evolution–a simple and efficient heuristic for global optimization over continuous spaces. J. Glob. Optim. 11, 341–359, https://doi.org/10.1023/A:1008202821328.
Tapiro, H., Oron-Gilad, T., Parmet, Y., 2016. Cell phone conversations and child pedestrian's crossing behavior; a simulator study. Saf. Sci. 89, 36–44, https://doi.org/10.1016/j.ssci.2016.05.013.
Tapiro, H., Oron-Gilad, T., Parmet, Y., 2020. Pedestrian distraction: The effects of road environment complexity and age on pedestrian's visual attention and crossing behavior. J. Safety Res. 72, 101–109, https://doi.org/10.1016/j.jsr.2019.12.003.
Tian, K., Markkula, G., Wei, C., Lee, Y.M., Madigan, R., Merat, N., Romano, R., 2022. Explaining unsafe pedestrian road crossing behaviours using a psychophysics-based gap acceptance model. Saf. Sci. 154, 105837, https://doi.org/10.1016/j.ssci.2022.105837.
van Ravenzwaaij, D., Oberauer, K., 2009. How to use the diffusion model: Parameter recovery of three methods: EZ, fast-dm, and DMAT. J. Math. Psych. 53 (6), 463–473, https://doi.org/10.1016/j.jmp.2009.09.004.
Vandekerckhove, J., Tuerlinckx, F., 2007. Fitting the ratcliff diffusion model to experimental data. Psychon. Bull. Rev. 14, 1011–1026, https://doi.org/10.3758/BF03193087.
Wagenmakers, E.-J., Van Der Maas, H.L., Grasman, R.P., 2007. An EZ-diffusion model for response time and accuracy. Psychon. Bull. Rev. 14 (1), 3–22, https://doi.org/10.3758/BF03194023.
Wiecki, T.V., Sofer, I., Frank, M.J., 2013. HDDM: Hierarchical Bayesian estimation of the drift-diffusion model in python. Front. Neuroinform. 7, 14, https://doi.org/10.3389/fninf.2013.00014.
Zgonnikov, A., Abbink, D., Markkula, G., 2022. Should I stay or should I go? Cognitive modeling of left-turn gap acceptance decisions in human drivers. Hum. Fact. https://doi.org/10.1177/00187208221144561, Advance online publication.
Zgonnikov, A., Beckers, N., George, A., Abbink, D., Jonker, C., 2023. Subtle motion cues by automated vehicles can nudge human drivers' decisions: Empirical evidence and computational cognitive model. PsyArXiv. http://dx.doi.org/10.31234/osf.io/3cu8b.
Zhao, J., Malenje, J.O., Tang, Y., Han, Y., 2019. Gap acceptance probability model for pedestrians at unsignalized mid-block crosswalks based on logistic regression. Accid. Anal. Prev. 129, 76–83, https://doi.org/10.1016/j.aap.2019.05.012.
Zito, G.A., Cazzoli, D., Jäger, M., Müri, R., Mosimann, U., Nyffeler, T., Mast, F., Nef, T., 2015. Street crossing behavior in younger and older pedestrians: an eye- and head-tracking study. BMC Geriatr. 15 (1), 1–10, https://doi.org/10.1186/s12877-015-0175-0.

Max Theisen received his MSc degree in Physics at the University of Bayreuth in 2019. He is currently working towards the PhD degree in Sensors & Cognitive Psychology at the Physics of Cognition group, Chemnitz University of Technology. Since 2020, he has been a research fellow at the Institute of Transportation Systems of the German Aerospace Center (DLR). His research interests include human cognition and behaviour in road traffic and human interaction with automated vehicles, particularly with respect to vulnerable road users.

Caroline Schießl received her diploma degree in psychology at the University of Würzburg in 2002 and her PhD in natural science at the Technical University of Braunschweig in 2009. Since 2003 she works at the DLR, Institute of Transportation Systems, as a team leader in the department "human factors" since 2007. In 2021 she became head of department "information flow modelling in mobility systems". Her research focuses on the development of research methods, techniques and tools to model, analyse, evaluate and design behaviour and interrelations among traffic participants, user-centred mobility services and solutions for connected, digitalized and automated future mobility.

Wolfgang Einhäuser studied physics in Heidelberg and Zurich, graduating from ETH Zurich in 2001. He did his PhD at the Institute of Neuroinformatics in Zurich, receiving his PhD from ETH in 2004. After postdoctoral research at Caltech (2005–2006) and at ETH (2007–2008), he was an assistant (W1) professor of Neurophysics at the University of Marburg from 2008 to 2015, with a 10-month stint as a resident fellow at the Center for Interdisciplinary Research (ZiF) in Bielefeld in 2012/2013. Since 2015 he has been a full professor for Physics of Cognition at Chemnitz University of Technology.

Gustav Markkula is Chair of Applied Behaviour Modelling at the Institute for Transport Studies, University of Leeds, UK. He obtained his MSc in Engineering Physics and Complex Adaptive Systems in 2004, and his PhD in Machine and Vehicle Systems in 2015, both from Chalmers University of Technology, Sweden. His main research interests are in cognitive and applied modelling of human perception, action, and interaction, especially in the context of road traffic.